isvr Institute of Sound and Vibration Research

Finite Element Analysis of Waveguides

L. Hinke, B. R. Mace and M.J. Brennan

ISVR Technical Memorandum No 932

April 2004

University of Southampton

SCIENTIFIC PUBLICATIONS BY THE ISVR

Technical Reports are published to promote timely dissemination of research results by ISVR personnel. This medium permits more detailed presentation than is usually acceptable for scientific journals. Responsibility for both the content and any opinions expressed rests entirely with the author(s).

Technical Memoranda are produced to enable the early or preliminary release of information by ISVR personnel where such release is deemed to the appropriate. Information contained in these memoranda may be incomplete, or form part of a continuing programme; this should be borne in mind when using or quoting from these documents.

Contract Reports are produced to record the results of scientific work carried out for sponsors, under contract. The ISVR treats these reports as confidential to sponsors and does not make them available for general circulation. Individual sponsors may, however, authorize subsequent release of the material.

UNIVERSITY OF SOUTHAMPTON

INSTITUTE OF SOUND AND VIBRATION RESEARCH

DYNAMICS GROUP

Finite Element Analysis of Waveguides

by

L. Hinke, B.R. Mace and M.J. Brennan

ISVR Technical Memorandum No: 932

April 2004

Authorised for issue by
Professor M.J. Brennan
Group Chairman

Abstract

Many structures present symmetry that can be used to simplify calculations. In this report, a method to estimate the wave motion in waveguides with uniform cross-section is presented. The commercial FE package ANSYS is used to model a section of the waveguide. The system matrices are then post-processed in MATLAB. The dynamic stiffness matrix is found, partitioned and rearranged to find the transfer matrix, which links the displacements and forces on both sides of the section. Wave propagation characteristics are described by the eigenvalues and eigenvectors of this matrix. The wavenumber dispersion relations, wavetypes and energy related quantities are calculated for examples of a rod, beam, plate strip and laminated plate. The main advantage of this approach, compared to other waveguide methods, is the use of a standard FE-package, so that the full power of existing element libraries can be used to model general structures. Also, the computational cost is independent of frequency, the post-processing algorithm is stable and can be made generic.

Contents

1 Introduction

1.1 Background

Structural vibrations in continuous systems can be described in terms of mode shapes and natural frequencies or in terms of wave motion [1–3]. For higher frequencies, especially the audio-frequency range, the wave approach is most appropriate, because the frequencies of concern are usually far above the fundamental structural frequencies and a large number of modes would have to be considered. The transmission of energy through a structure, for example from a source to a receiver, can be easily described in terms of waves using the phenomena of interference, reflection, diffraction and scattering. The modal solution is a global approach, because each mode depends on the structure as a whole, with all its parts and the boundary conditions. The number of modes is infinite for the structure, but there is only a finite number in a finite frequency range. In general, the motion of a structure can be considered as the sum of modal contributions. In contrast, the wave approach is a local approach, because only the properties at a point of the structure are needed to determine the wave propagation characteristics at this point. The different viewpoints of vibration are compared by a simple example in section 1.2

At low frequencies, a classical finite element model can be used to describe the wave motion of a structure. There is a requirement of using 6-10 finite elements per wavelength in order to get accurate results. At higher frequencies, the wavelengths becomes very small and this results in a computationally expensive FE-model. It is possible to reduce the computational load by using symmetry. Additionally, methods have been developed that use a FE-model with a size independent of frequency. One of such methods is the use of waveguide models. Alternatively, a statistical analysis can be appropriate for high frequency vibration, which is also unaffected by uncertainties in the structure. One such approach is statistical energy analysis (SEA) [4,5], where a structure is modelled as a number of connected subsystems and the frequency averaged energy-flow between them is considered. However, the properties of the subsystems can still be found using wave analysis.

1.2 Wave and modal solutions for continuous systems

Continuous systems are characterized by continuously distributed mass and stiffness properties. They also deform continuously and therefore have an infinite number of degrees of freedom. The motion of such structures is described by partial differential equations. To illustrate the modal and wave approach, a simple one-dimensional

partial differential equation of motion will be used. It is given in the form [1,6]

$$\frac{\partial^2 u}{\partial t^2} = c^2 \frac{\partial^2 u}{\partial x^2} \tag{1.2.1}$$

Equations of this form described for example axial vibrations of a rod, torsional vibrations of a shaft and sound waves in air.

1.2.1 Modal approach

A solution to equation 1.2.1 can be found by separation of the variables (method of Bernoulli)

$$u(x,t) = w(x)p(t) \tag{1.2.2}$$

Considering harmonic motion, two ordinary differential equations for time and spatial dependence can be found as

$$\ddot{p}(t) + \omega^2 p(t) = 0 \tag{1.2.3}$$

$$w''(x) + \frac{\omega^2}{c^2} w(x) = 0 \tag{1.2.4}$$

Solutions can be written in the form

$$p(t) = T_s sin(\omega t) + T_c cos(\omega t) = T e^{i\omega t} \tag{1.2.5}$$

$$w(x) = A sin((\omega/c)\ x) + B cos((\omega/c)\ x) \tag{1.2.6}$$

The initial conditions are used to determine the constants T and the boundary conditions are used to determine the constants A and B. As an example, if the field variable u is fixed at the two ends $x = 0$ and $x = L$ of the one-dimensional system, the boundary conditions are

$$u(0,t) = w(0,t) = 0 \qquad u(l,t) = w(l,t) = 0 \tag{1.2.7}$$

Substituting in equation 1.2.6 gives

$$A sin(\frac{wl}{c}) = 0 \tag{1.2.8}$$

which is satisfied for all $\omega_n = (n\pi c)/l$ since $A \neq 0$. Thus it follows that

$$w_n(x) = A_n sin(\frac{n\pi x}{l}) \tag{1.2.9}$$

is the nth modeshape of the system at the nth natural frequency ω_n. The free vibration of the system can be expressed as a modal superposition of the vibrations in each mode, i.e.

$$u(x,t) = \sum_{n=1}^{\infty} \tilde{A}_n\ sin(\frac{n\pi x}{l})\ e^{i\omega_n t} \tag{1.2.10}$$

1.2.2 Wave approach

The solution to equation 1.2.1 can be expressed as

$$u(x,t) = f_1(ct - x) + f_2(ct + x) \tag{1.2.11}$$

where f_1 and f_2 are arbitrary functions which represent waves going in the positive and negative x-directions respectively (method of d'Alembert). For time harmonic motion at at frequency ω, the solution to equation 1.2.6 can be written as

$$w(x) = Ae^{-ikx} + Be^{ikx} \tag{1.2.12}$$

where $k = \omega/c = 2\pi/\lambda_L$ is the wavenumber and represents the number of wavelengths per 2π-metres. Together with equation 1.2.5 and $\tilde{A} = TA$, $\tilde{B} = TB$ it follows that

$$u(x,t) = \tilde{A}e^{i(\omega t - kx)} + \tilde{B}e^{i(\omega t + kx)} \tag{1.2.13}$$

which is in the form of equation 1.2.11 and shows the difference of this approach to the modal approach (equation 1.2.10). The wavenumber k depends on the local wave speed c and on frequency ω.

The comparison to modes shapes can be done by looking at the reflection of the wave at the boundaries. For a fixed end $u = 0$ it follows that $\tilde{B} = -\tilde{A}$. Therefore equation 1.2.13 simplifies to

$$u(x,t) = 2\tilde{A}i\ sin(kx)\ e^{i\omega t} \tag{1.2.14}$$

where $sin(kx)$ describes a standing wave, which compares to a mode of vibration. The wavenumber k and the frequency ω of a standing wave can be found by looking at the total phase change experienced by a wave as it travels around the system. Natural frequencies occur in the case of phase closure when the phase change is a multiple of 2π. For a waveguide of length l with fixed ends, it follows that

$$kl + \pi + kl + \pi = 2kl + 2\pi = m2\pi \quad \longrightarrow \quad kl = n\pi \tag{1.2.15}$$

Therefore

$$\omega_n = k_n c = \frac{n\pi c}{l}$$

which is the same as found by the modal approach.

1.3 Waveguides

In general, a waveguide is a medium confined by parallel boundaries that allows wave propagation in the direction of the waveguide only (Figure 1.1) [1,7]. Waves spreading out in various directions are multiply reflected at the boundaries and transformed into waves propagating in the direction of the waveguide axis. These guided waves involve a characteristic (modal) distribution of the wave variable over the cross-section of the waveguide, which is based on the interference of the reflected waves.

In this report, the waveguide is assumed to have a uniform cross-section, which means that the cross-section has the same physical and geometrical properties at all points along the axis of wave propagation. Waves can propagate in both directions along the waveguide and the cross-section can be 0,1 or 2 dimensional. Examples

for a 0-dimensional cross-section are a rod undergoing axial vibrations or a beam in bending. The displacement $u(x)$ is then a function of x only and therefore constant across the cross-section. In this report, the focus will be on waveguides with one-dimensional cross-sections, such as a plate strip in bending (Figure 1.2) or an infinite plate. The displacement $u(x, y)$ is a function of the coordinate x along the direction of wave propagation and the coordinate y, which describes the characteristic shape over the cross-section. An extruded section, an acoustic duct and a tyre are examples of waveguides with 2-dimensional cross-sections. For the tyre, the waveguide axis is circular rather than a straight line (Figure 1.3).

Depending on the constraints that the boundaries impose upon the wave motion, there is a minimum frequency (resonance) for each wave mode to start propagating, the so called cut-on or cut-off frequency. Below that frequency, a mode cannot propagate energy and the amplitude decays exponentially.

1.4 Previous work

Many structures in reality are uniform in one direction. Structures with translational or rotational uniformity and a constant cross-section are referred to as waveguides. Structures with periodic symmetry, which means that a characteristic non-constant cross-section repeats periodically, are referred to as periodic structures and also exhibit waveguide behaviour. All work that considers such structures have the common goal to make use of the symmetry to simplify calculations [8, 9].

For simple waveguide structures, the wave approach can be used to find an analytical solution. For more general structures, the displacements in the cross-section can be described by a finite element model while the variation along the waveguide axis is expressed by an ordinary differential equation. This approach has been called dynamic stiffness method [10] or also the spectral finite element method [11]. Compared to classical methods, the FE model is now one dimension smaller, because only the cross-section has to be meshed. Motion along the waveguide is assumed to vary as e^{-ikx}, where k is the wavenumber. The characteristic finite element equation for the cross-section can be put in the form [12]

$$\left(\mathbf{K}(k) - \omega^2\mathbf{M}\right)\mathbf{q} = 0 \tag{1.4.1}$$

where $\mathbf{q}$ is the displacement vector of the cross-section and $\mathbf{M}$ is the mass matrix. The stiffness matrix $\mathbf{K}(k)$ is developed for various powers of the wavenumber k as

$$\mathbf{K}(k) = \sum_i \mathbf{K}_i(k)^i \tag{1.4.2}$$

where the matrices $\mathbf{K}_i$ are independent of wavenumber. However these are not standard FE matrices and must be determined for each application separately using methods such as Hamilton's principle [13–15]. The dispersion relations can be obtained by calculating the frequencies for different given wavenumbers.

Another method, that has been used mainly to estimate wave propagation in periodic structures, is the transfer matrix approach [9, 16]. Wave propagation can be described by propagation constants λ as well as by a transfer matrix $\mathbf{T}$, which relates the displacements $\mathbf{q}$ and forces $\mathbf{f}$ from the left border to the right border of a

periodic element. This can be written in the form

$$\begin{bmatrix} \mathbf{q}_R \\ -\mathbf{f}_R \end{bmatrix} = \mathbf{T} \begin{bmatrix} \mathbf{q}_L \\ -\mathbf{f}_L \end{bmatrix} = \lambda \begin{bmatrix} \mathbf{q}_L \\ \mathbf{f}_L \end{bmatrix} \tag{1.4.3}$$

which is an eigenvalue problem. The propagation constants λ are eigenvalues of the transfer matrix $\mathbf{T}$ and can be written as $\lambda = e^{ikl}$ where k is the wavenumber and l is the length of the periodic element. The dispersion relations are obtained by calculating the wavenumber for a given frequency. This is called the reverse problem [17, 18], because it is opposite to the spectral element approach. However, previous works using this approach mainly deal with simple structures and the solutions are found analytically.

1.5 Present report

Recently, Duhamel [19] showed how to use the transfer matrix approach to estimate the wave motion in periodic structures and waveguide structures using models that come from standard FE-packages. This report is intended to extend this work and to apply the methods developed in [19] to various situations.

The FE-software ANSYS is used to obtain the system matrices for a cross-section of a waveguide. The mass, stiffness and damping matrices are then post-processed in MATLAB. The dynamic stiffness matrix is calculated, partitioned and rearranged to find the transfer matrix $\mathbf{T}$. Wave propagation characteristics are described by the eigenvalues and eigenvectors of this matrix. Special attention is given to show how the eigenvalues of $\mathbf{T}$ relate to propagating, attenuating and evanescent waves. The wavenumber dispersion relations, wavetypes and energy related quantities are calculated for different examples.

The main advantage of the approach compared to the spectral element method is the use of a standard FE-package, so that the full power of existing element libraries can be used. The computational cost is also independent of frequency, because the finite element mesh of the cross-section requires only one element in the direction of wave propagation.

The individual sections of this report address the following points:

Section 2 describes the finite element approach and the wave analysis.

Section 3 considers bending waves in a beam. Firstly, the analytical solution for bending waves in beams is derived using an Euler-Bernoulli-Beam. Secondly, the methods presented in section 2 are applied. The standard mass and stiffness matrices for a beam are well known and therefore the numerical solution is straightforward. Finally, an experiment to measure the wavenumber in a beam is described and the results are compared with analytical and numerical solutions.

Section 4 considers bending waves in infinite plates and free and simply supported plate strips. The section of the waveguide to be modelled in the FE-software is defined and the properties of the FE-mesh and the use of different element types are discussed. A simple two element mesh with 10 degrees of freedom is used to give a clear understanding of how the eigenvalues of the transfer matrix relate

to propagating, attenuating or evanescent waves. Therefore, the location and the locus of the eigenvalues in different complex planes are visualized. Then a 50 element mesh is used to calculate the dispersion curves and the results are compared to the two element case as well as to the analytical solution derived from the wave equation for a beam in bending. For the simply supported plate, the mode shapes are obtained from the eigenvectors and the cut-on condition is discussed. Finally, the kinetic and potential energies, the power-flow and the group velocity are calculated for each wave-type and their physical meanings are discussed.

Section 5 shows the application of the previously discussed methods and techniques to the advanced example of a laminated plate strip. Special phenomena like the cut-on of waves with finite wavenumbers and the existence of waves only over a certain frequency range are discussed in detail.

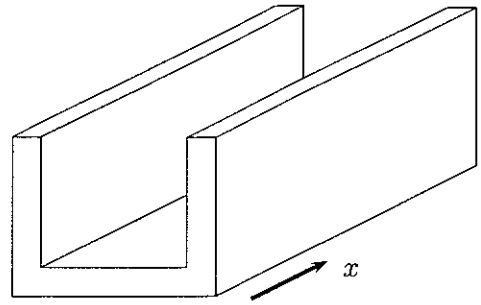

FIGURE 1.1: *Waveguide with uniform cross-section*

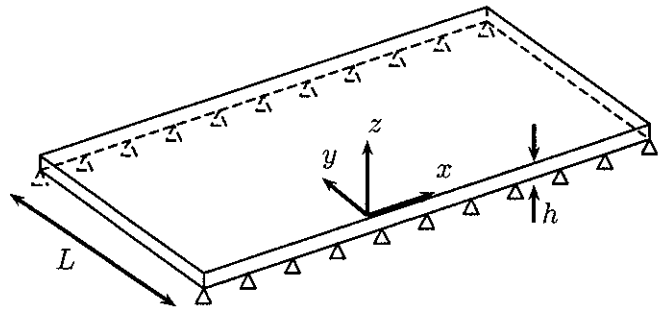

FIGURE 1.2: *Simply supported plate strip with height h and width L*

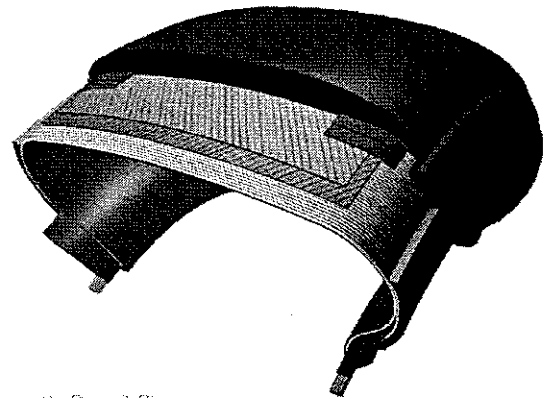

FIGURE 1.3: *Cross-section of a tyre*

2 FINITE ELEMENT ANALYSIS OF WAVE MOTION

2.1 Modelling of a section of a waveguide

In section 1, waveguides with 0,1 and 2-dimensional cross-sections have been introduced. In order to predict the characteristics of the wave motion, a section of the waveguide will be modelled using conventional FE methods. A condition for the wave analysis is to have an equal number and identical distribution of degrees of freedom on each side of the section. Figure 2.1 shows a 3-element mesh over a 1-dimensional cross-section using rectangular 4-node elements.

Depending on the application, the nodes will have different numbers of degrees of freedom giving linear, quadratic or cubic shape functions. In the direction of wave propagation a length Δ is covered by one finite element. To obtain good results in the wave analysis, the length Δ should be less then one sixth of the expected wavelength. This corresponds to the more familiar requirement of using 6-10 elements per wavelength. However, if the length Δ is very short compared to the longest wavelength, computational problems will arise [19]. The number of elements over the cross-section has to be high enough to characterize the wavemode. The higher the order of the wavemode, the more elements and degrees of freedom are needed to get good results. The width-to-height ratio should comply with standard modelling techniques.

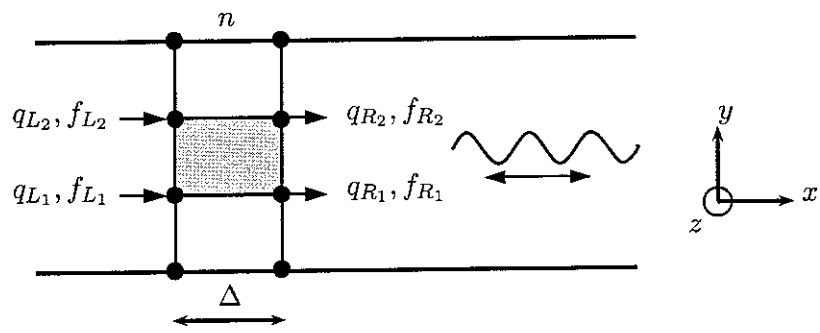

FIGURE 2.1: *Finite element mesh of cross-section*

The equation of motion of the section can be found in the form of

$$\mathbf{M}\ddot{\mathbf{q}} + \mathbf{C}\dot{\mathbf{q}} + \mathbf{K}\mathbf{q} = \mathbf{f} \tag{2.1.1}$$

Substituting $\dot{\mathbf{q}} = i\omega\mathbf{q}$ and $\ddot{\mathbf{q}} = -\omega^2\mathbf{q}$ gives

$$(\mathbf{K} + i\omega\mathbf{C} - \omega^2\mathbf{M})\mathbf{q} = \mathbf{f} \tag{2.1.2}$$

where $\mathbf{q}$ is the displacement vector containing all degrees of freedom and $\mathbf{f}$ is the loading vector containing the nodal loads. The stiffness matrix $\mathbf{K}$, the mass matrix $\mathbf{M}$ and the damping matrix $\mathbf{C}$ can be combined to a dynamic stiffness matrix $\mathbf{D}(\omega) = (\mathbf{K}+i\omega\mathbf{C}-\omega^2\mathbf{M})$, which depends on frequency. The equation of motion of the section now becomes

$$\mathbf{D}(\omega)\mathbf{q} = \mathbf{f} \tag{2.1.3}$$

After partitioning the displacement vector $\mathbf{q}$ and the loading vector $\mathbf{f}$ into their left and right components $\mathbf{q}_L$, $\mathbf{f}_L$ and $\mathbf{q}_R$, $\mathbf{f}_R$ respectively, equation 2.1.3 can be written in the form

$$\begin{bmatrix} \mathbf{D}_{LL} & \mathbf{D}_{LR} \\ \mathbf{D}_{RL} & \mathbf{D}_{RR} \end{bmatrix} \begin{bmatrix} \mathbf{q}_L \\ \mathbf{q}_R \end{bmatrix} = \begin{bmatrix} \mathbf{f}_L \\ \mathbf{f}_R \end{bmatrix} \tag{2.1.4}$$

The dynamic stiffness matrix $\mathbf{D}$ is symmetric, hence the sub-matrices $\mathbf{D}_{LL}$ and $\mathbf{D}_{RR}$ are also symmetric and $\mathbf{D}_{LR}^T = \mathbf{D}_{RL}$. If n is the number of the degrees of freedom, $\mathbf{D}$ is a $n \times n$ matrix and the submatrices are of size $n/2 \times n/2$.

Duhamel [19] shows how to calculate the dynamic stiffness matrix for periodic structures. Several cells in the direction of the wave propagation are considered and left and right propagation matrices are introduced. Finally, a global dynamic stiffness matrix can be calculated with a computational cost that is independent of the number of cells.

2.2 Transfer matrix approach

We introduce a transfer matrix $\mathbf{T}$ that relates the displacements and forces between two adjacent cells n and $n+1$ along the direction of wave propagation. In terms of the nodal values at the left border of each cell this can be expressed as

$$\begin{bmatrix} \mathbf{q}_L^{n+1} \\ \mathbf{f}_L^{n+1} \end{bmatrix} = \mathbf{T} \begin{bmatrix} \mathbf{q}_L^{n} \\ \mathbf{f}_L^{n} \end{bmatrix} \tag{2.2.1}$$

In the case of a uniform cross-section and no external loads applied, the following continuity and equilibrium conditions are satisfied at the nodes connecting two cells:

$$\begin{bmatrix} \mathbf{q}_L^{n+1} \\ \mathbf{f}_L^{n+1} \end{bmatrix} = \begin{bmatrix} \mathbf{q}_R^{n} \\ -\mathbf{f}_R^{n} \end{bmatrix} \tag{2.2.2}$$

Therefore equation 2.2.2 can be written in the form

$$\begin{bmatrix} \mathbf{q}_R \\ -\mathbf{f}_R \end{bmatrix} = \mathbf{T} \begin{bmatrix} \mathbf{q}_L \\ \mathbf{f}_L \end{bmatrix} \tag{2.2.3}$$

relating now the left and right nodal values within one cell to each other.

From the first row of equation 2.1.4 it follows that

$$\mathbf{D}_{LL}\mathbf{q}_L + \mathbf{D}_{LR}\mathbf{q}_R = \mathbf{f}_L \tag{2.2.4}$$

$$\mathbf{q}_R = \begin{bmatrix} -\mathbf{D}_{LR}^{-1}\mathbf{D}_{LL} & \mathbf{D}_{LR}^{-1} \end{bmatrix} \begin{bmatrix} \mathbf{q}_L \\ \mathbf{f}_L \end{bmatrix} \tag{2.2.5}$$

The second row of equation 2.1.4 with equation 2.2.5 substituted gives

$$\mathbf{D}_{RL}\mathbf{q}_L + \mathbf{D}_{RR}\mathbf{q}_R = \mathbf{f}_R \tag{2.2.6}$$

hence

$$\mathbf{f}_R = \begin{bmatrix} \mathbf{D}_{RL} - \mathbf{D}_{RR}\mathbf{D}_{LR}^{-1}\mathbf{D}_{LL} & \mathbf{D}_{RR}\mathbf{D}_{LR}^{-1} \end{bmatrix} \begin{bmatrix} \mathbf{q}_L \\ \mathbf{f}_L \end{bmatrix} \tag{2.2.7}$$

From equations 2.2.3, 2.2.5 and 2.2.7 it follows that

$$\mathbf{T} = \begin{bmatrix} -\mathbf{D}_{LR}^{-1}\mathbf{D}_{LL} & \mathbf{D}_{LR}^{-1} \\ -\mathbf{D}_{RL} + \mathbf{D}_{RR}\mathbf{D}_{LR}^{-1}\mathbf{D}_{LL} & -\mathbf{D}_{RR}\mathbf{D}_{LR}^{-1} \end{bmatrix} \tag{2.2.8}$$

Thus the transfer matrix depends only on the dynamic stiffness matrix of one cell.

2.3 Free wave propagation and eigenvalue problem

When a free wave travels along the waveguide, the displacements and forces at different cross-sections differ only by a propagation factor. Using the borders of two adjacent cells and introducing the factor λ, we can express this in the form

$$\begin{bmatrix} \mathbf{q}_L^{n+1} \\ \mathbf{f}_L^{n+1} \end{bmatrix} = \begin{bmatrix} \mathbf{q}_R^{n} \\ -\mathbf{f}_R^{n} \end{bmatrix} = \lambda \begin{bmatrix} \mathbf{q}_L^{n} \\ \mathbf{f}_L^{n} \end{bmatrix} \tag{2.3.1}$$

In more detail, the factor λ relates to a change in wave amplitude and a change in phase over a certain length, in this case over the length of a cell Δ. Substituting equation 2.2.1 or 2.2.3 in equation 2.3.1 gives the eigenvalue problem

$$\begin{aligned} \mathbf{T} \begin{bmatrix} \mathbf{q}_L^{n} \\ \mathbf{f}_L^{n} \end{bmatrix} &= \lambda \begin{bmatrix} \mathbf{q}_L^{n} \\ \mathbf{f}_L^{n} \end{bmatrix} \\ [\mathbf{T} - \lambda I] \begin{bmatrix} \mathbf{q}_L \\ \mathbf{f}_L \end{bmatrix} &= 0 \end{aligned} \tag{2.3.2}$$

where the superscript n can be omitted.

Substituting $\mathbf{q}_R = \lambda \mathbf{q}_L$ and $\mathbf{f}_R = -\lambda \mathbf{f}_L$ in equation 2.2.4 and equation 2.2.6 gives

$$\mathbf{D}_{LL}\mathbf{q}_L + \mathbf{D}_{LR}\lambda\mathbf{q}_L = \mathbf{f}_L \tag{2.3.3}$$

$$\mathbf{D}_{RL}\mathbf{q}_L + \mathbf{D}_{RR}\lambda\mathbf{q}_L = -\lambda\mathbf{f}_L \tag{2.3.4}$$

which can be written in matrix form as

$$\begin{bmatrix} \mathbf{D}_{LL} + \lambda\mathbf{D}_{LR} & -I \\ \mathbf{D}_{RL} + \lambda\mathbf{D}_{RR} & \lambda I \end{bmatrix} \begin{bmatrix} \mathbf{q}_L \\ \mathbf{f}_L \end{bmatrix} = 0 \tag{2.3.5}$$

Nonzero solutions to equation 2.3.5 only exist if the matrix is singular, therefore the determinant has to be zero.

$$\det \begin{bmatrix} \mathbf{D}_{LL} + \lambda \mathbf{D}_{LR} & -I \\ \mathbf{D}_{RL} + \lambda \mathbf{D}_{RR} & \lambda I \end{bmatrix} = 0 \tag{2.3.6}$$

$$\lambda \mathbf{D}_{LL} + \lambda^2 \mathbf{D}_{LR} + \mathbf{D}_{RL} + \lambda \mathbf{D}_{RR} = 0 \tag{2.3.7}$$

$$\mathbf{D}_{LL} + \lambda \mathbf{D}_{LR} + \frac{1}{\lambda} \mathbf{D}_{RL} + \mathbf{D}_{RR} = 0 \tag{2.3.8}$$

Taking the transpose of equation 2.3.8 and noting the symmetry conditions $\mathbf{D}_{LL}^T = \mathbf{D}_{LL}, \mathbf{D}_{RR}^T = \mathbf{D}_{RR}$ and $\mathbf{D}_{LR}^T = \mathbf{D}_{RL}$ gives a further equation as

$$\mathbf{D}_{LL} + \frac{1}{\lambda} \mathbf{D}_{LR} + \lambda \mathbf{D}_{RL} + \mathbf{D}_{RR} = 0 \tag{2.3.9}$$

By comparing equation 2.3.8 and equation 2.3.9 it follows that if λ is an eigenvalue, then $\frac{1}{\lambda}$ is an eigenvalue as well.

The same relations can also be obtained by substituting equation 2.3.3 into equation 2.3.4 which gives directly

$$\left(\mathbf{D}_{LL} + \frac{1}{\lambda} \mathbf{D}_{LR} + \lambda \mathbf{D}_{RL} + \mathbf{D}_{RR} \right) \mathbf{q}_L = 0 \tag{2.3.10}$$

This formulation is also known as a polynomial eigenvalue problem, where the eigenvalue λ appears in different powers.

2.3.1 Eigenvalues

The n eigenvalues come in m independent pairs, where $m = n/2$ is the number of degrees of freedom on each side of the cross-section. The set of m eigenvalues given by $|\lambda_i| < 1$ describes waves travelling in the positive direction, the set of m eigenvalues given by $|\lambda_i| > 1$ describes waves travelling in the negative direction. In general the eigenvalues are complex and can be written as

$$\lambda_j = e^{-\mu_j \Delta} e^{-ik_j \Delta} \tag{2.3.11}$$

with $i = \sqrt{-1}$, $\mu \in \mathbf{R}$ represents the change in amplitude and $k \in \mathbf{R}$ represents the change in phase, which has been previously introduced as the wavenumber. The signs have been chosen in such a way that μ and k are positive for waves travelling in the positive direction. A more convenient way to present numerical results can be found by using a complex number with real part μ and imaginary part k. Equation 2.3.11 is therefore rewritten such that

$$-\frac{ln\lambda_j}{\Delta} = \mu_j + ik_j \tag{2.3.12}$$

In the absence of damping, which will be assumed from now on, the amplitude of propagating waves remains constant, which is given by $|\lambda_j| = 1$ and $\mu_j = 0$ and $\lambda_j = e^{-ik\Delta}$ since

$$|e^{ix}| = 1 \qquad \text{for all } x \in \mathbf{R} \tag{2.3.13}$$

The direction of wave propagation is determined by the direction of power-flow.

λ	$\lvert\lambda\rvert$	μ	k	wave	direction	index
imaginary	1	0	>0	propagating		a
real	<1	>0	0	evanescent	positive	b
complex	<1	>0	>0	attenuating		c
imaginary	1	0	<0	propagating		d
real	>1	<0	0	evanescent	negative	e
complex	>1	<0	<0	attenuating		f

TABLE 2.1: Properties of eigenvalues and associated waves

For attenuating or evanescent waves, given by $|\lambda_j| \lesseqgtr 1$, the amplitude decreases in the direction of wave propagation. The amplitude of an evanescent wave decays rapidly without oscillation by a factor of $e^{-\mu\Delta}$ over the length Δ. An attenuating wave oscillates with the wavenumber k and the amplitude decays at the same time by $e^{-\mu\Delta}$.

The different types of waves are summarized in Table 2.1 and Figure 2.2. The properties of waves can be related to the location of the eigenvalues in the complex λ-plane (equation 2.3.11) and in the complex (μ, k)-plane (equation 2.3.12). A corresponding visualization is given by Figure 2.3.

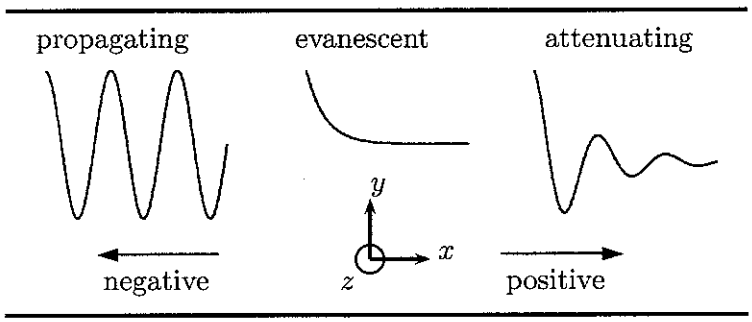

FIGURE 2.2: *Different types of waves*

2.3.2 Eigenvectors

The jth eigenvector, calculated from the eigenvalue problem (2.3.2), is of size n and contains a set of m displacements $\mathbf{q}_{j_L}$ and and a set of m forces $\mathbf{f}_{j_L}$ associated with the left border of the cell. The nodal displacements and forces at the right border of the cell can be obtained using equation 2.3.1 and are given by

$$\mathbf{q}_{j_R} = \lambda \mathbf{q}_{j_L} \qquad \mathbf{f}_{j_R} = -\lambda \mathbf{f}_{j_L}$$

The change of the eigenvectors of the jth wavemode over an arbitrary distance D

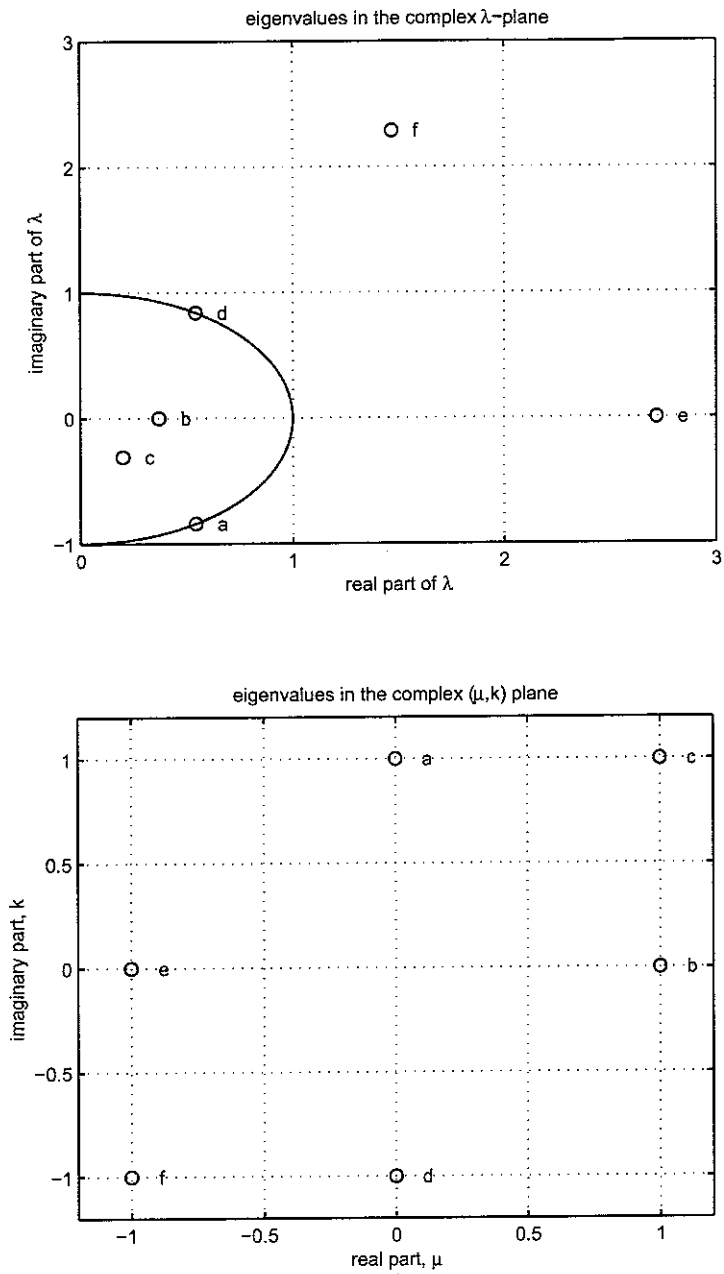

FIGURE 2.3: *Location of eigenvalues in complex λ-plane and complex μ, k-plane.*

along the direction of wave propagation is given by

$$\begin{bmatrix} \mathbf{q}_{j_L} \\ \mathbf{f}_{j_L} \end{bmatrix}_{(x+D)} = \lambda_j^{(\frac{D}{\Delta})} \begin{bmatrix} \mathbf{q}_{j_L} \\ \mathbf{f}_{j_L} \end{bmatrix}_{(x)}$$

If the polynomial eigenvalue problem 2.3.10 is solved, the jth eigenvector only contains a set of m displacements $\mathbf{q}_{j_L}$. The associated forces can then be found by equation 2.2.4.

$$\mathbf{f}_{j_L} = (\mathbf{D}_{LL} + \lambda \mathbf{D}_{LR})\mathbf{q}_{j_L} \tag{2.3.14}$$

The characteristic displacement of the cross-section of the waveguide, associated with the jth wavemode, is given by the nodal displacements at the left and right border and will be denoted by

$$\Phi_j = \begin{bmatrix} \mathbf{q}_{j_L} \\ \mathbf{q}_{j_R} \end{bmatrix} = \begin{bmatrix} \mathbf{q}_{j_L} \\ \lambda_j \mathbf{q}_{j_L} \end{bmatrix} \tag{2.3.15}$$

Similarly to the eigenvalues, the n eigenvectors can also be split into two sets of m eigenvectors, one associated with waves travelling in the positive direction and one with waves travelling in the negative direction. Therefore we define

$$\begin{bmatrix} \mathbf{q}^+_{j_L} \\ \mathbf{f}^+_{j_L} \end{bmatrix} \qquad \text{for } |\lambda_j| \leq 1$$

$$\begin{bmatrix} \mathbf{q}^-_{j_L} \\ \mathbf{f}^-_{j_L} \end{bmatrix} \qquad \text{for } |\lambda_j| \geq 1$$

The general wave motion in the waveguide is then given by a linear combination of the eigenvectors with amplitudes a_j.

$$\begin{bmatrix} \mathbf{q}_L \\ \mathbf{f}_L \end{bmatrix} = \sum_{j=1}^{m} \left(a_j^+ \begin{bmatrix} \mathbf{q}^+_{j_L} \\ \mathbf{f}^+_{j_L} \end{bmatrix} + a_j^- \begin{bmatrix} \mathbf{q}^-_{j_L} \\ \mathbf{f}^-_{j_L} \end{bmatrix} \right) \tag{2.3.16}$$

2.4 Energy related quantities

2.4.1 Kinetic, potential and total energy of waves

The energy related quantities in this section always refer to one wave, therefore the subindex j will be left out in order to simplify the equations.

The kinetic energy of a mass m is given by

$$E_{kin} = \frac{1}{2} m v^2 = \frac{1}{2} m \dot{q}^2 \tag{2.4.1}$$

Using complex notation, the time-average kinetic energy can be written as

$$\bar{E}_{kin} = \frac{1}{2} m \frac{1}{2} \mathrm{Re}\{\dot{q}^* \dot{q}\} = \frac{1}{4} m \mathrm{Re}\{(i\omega q)^* (i\omega q)\} = \frac{1}{4} m \omega^2 |q|^2 \tag{2.4.2}$$

where $*$ denotes the complex conjugate.

The potential energy of an element with stiffness k is given by

$$E_{pot} = \frac{1}{2} k q^2 \tag{2.4.3}$$

Similarly to equation 2.4.2, the time-average potential energy can be found as

$$\bar{E}_{pot} = \frac{1}{2}k\frac{1}{2}\mathrm{Re}\{q^* q\} \tag{2.4.4}$$

In order to find the time-average kinetic and potential energies of the section n of the waveguide under the passage of a wave, the previous equations can be written in matrix form using the mass and stiffness matrices and the displacement vector of the section. Thus

$$\bar{E}^n_{kin} = \frac{1}{4}\mathrm{Re}\{(i\omega\Phi)^H \mathbf{M}(i\omega\Phi)\} \tag{2.4.5}$$

$$\bar{E}^n_{pot} = \frac{1}{4}\mathrm{Re}\{\Phi^H \mathbf{K}\Phi\} \tag{2.4.6}$$

where Φ is defined in equation 2.3.15 and H now denotes the conjugate transpose. The time-average total energy associated with a section is then given by

$$\bar{E}^n_{tot} = \bar{E}^n_{kin} + \bar{E}^n_{pot} \tag{2.4.7}$$

Furthermore the time-average total energy per unit length is

$$\underline{\bar{E}}_{tot} = \frac{\bar{E}^n_{tot}}{\Delta} \tag{2.4.8}$$

2.4.2 Power-flow and group velocity

The transmitted power at a point is given by

$$P = f\dot{q} \tag{2.4.9}$$

Using complex notation, the time average power-flow is given by

$$\bar{P} = \frac{1}{2}\mathrm{Re}\{f^*(i\omega q)\} \tag{2.4.10}$$

The power-flow through the section of the waveguide can be calculated either at the left or at the right border. The power-flow is constant for freely propagating waves and positive in the direction of wave propagation. It is given by

$$\bar{P} = \frac{1}{2}\mathrm{Re}\{\mathbf{f}^H_L i\omega \mathbf{q}_L\} = \frac{1}{2}\mathrm{Re}\{-\mathbf{f}^H_R i\omega \mathbf{q}_R\} \tag{2.4.11}$$

The speed at which energy travels along the waveguide is called the group velocity c_g and is defined by

$$\bar{P} = \underline{\bar{E}}_{tot} c_g \qquad c_g = \frac{\bar{P}}{\underline{\bar{E}}_{tot}} \tag{2.4.12}$$

The preceding equations show a simple way to calculate the group velocity, which is an important parameter for many applications where noise and vibration transmission are of interest, i.e. statistical energy analysis.

3 WAVE PROPAGATION IN BEAMS

3.1 Analytical solution

The equation of motion or the wave equation of a beam in bending is (see Cremer [3], Fahy [1])

$$EI\frac{\partial^4 w}{\partial x^4} + \rho A\frac{\partial^2 w}{\partial t^2} \tag{3.1.1}$$

where E is the Young's modulus, I the moment of inertia, ρ the density, A the cross-sectional area and w the transverse displacement. Substitution of the expression for a propagating wave $w(x,t) = ae^{-ikx}e^{i\omega t}$ yields

$$EIk^4 - \rho A\omega^2 = 0 \tag{3.1.2}$$

where k is the wavenumber

$$k^4 = \frac{\rho A}{EI}\omega^2 \tag{3.1.3}$$

Equation 3.1.3 has four roots, which are in the form of k, $-k$, ik and $-ik$. Therefore, a general solution to equation 3.1.1 can be written in the form

$$w(x,t) = \left(Ae^{-ikx} + Be^{ikx} + Ce^{-kx} + De^{kx}\right)e^{i\omega t}$$

or

$$w(x,t) = Ae^{-ikx+i\omega t} + Be^{ikx+i\omega t} + Ce^{-kx+i\omega t} + De^{kx+i\omega t} \tag{3.1.4}$$

The terms associated with A and B in equation 3.1.4 represent waves that propagate in the positive and negative direction respectively. The other two terms represent evanescent waves that decay exponentially with distance. Therefore, the solution to the bending wave equation in a beam can be expressed as a linear combination of four waves.

3.2 Finite element solution

The mass and stiffness matrices for a beam element of length l are (see Petyt [20])

$$\mathbf{K} = \frac{EI}{l^3}\begin{bmatrix} 12 & 6l & -12 & 6l \\ 6l & 4l^2 & -6l & 2l^2 \\ -12 & -6l & 12 & -6l \\ 6l & 2l^2 & -6l & 4l^2 \end{bmatrix} \qquad \mathbf{M} = \frac{\rho Al}{420}\begin{bmatrix} 156 & 22l & 54 & -13l \\ 22l & 4l^2 & 13l & -3l^2 \\ 54 & 13l & 156 & -22l \\ -13l & -3l^2 & -22l & 4l^2 \end{bmatrix}$$

The dynamic stiffness matrix is $\mathbf{D} = \mathbf{K} - \omega^2\mathbf{M}$. The transfer matrix is then given by

$$\mathbf{T} = \begin{bmatrix} -\mathbf{D}_{LR}^{-1}\mathbf{D}_{LL} & \mathbf{D}_{LR}^{-1} \\ -\mathbf{D}_{RL} + \mathbf{D}_{RR}\mathbf{D}_{LR}^{-1}\mathbf{D}_{LL} & -\mathbf{D}_{RR}\mathbf{D}_{LR}^{-1} \end{bmatrix}$$

where $\mathbf{D}_{LL}$, $\mathbf{D}_{LR}$, $\mathbf{D}_{RL}$ and $\mathbf{D}_{RR}$ are the 2×2 submatrices of $\mathbf{D}$. The matrix $\mathbf{T}$ has four degrees of freedoms and therefore the solution of the eigenvalue problem $[\mathbf{T} - \lambda I]\mathbf{q} = 0$ has also four eigenvalues. They are such that

$$|\lambda_1| = |\lambda_2| = 1 \qquad \lambda_1^* = \lambda_2$$

$$\lambda_3 \in \mathbf{R}, \quad \lambda_4 \in \mathbf{R}, \qquad \lambda_3 = \frac{1}{\lambda_4}$$

In the complex (μ, k)-plane the four eigenvalues are given by

$$\begin{array}{llll} k_1 > 0, & k_2 < 0; & \mu_1 = \mu_2 = 0; & k_1 = -k_2 = \mu_3 = -\mu_4 \\ \mu_3 > 0, & \mu_4 < 0; & k_3 = k_4 = 0; & \end{array}$$

The four eigenvalues represent the four waves from solution 3.1.4, whereby λ_1 and λ_2 are the waves propagating in the positive and negative direction respectively and λ_3 and λ_4 are the evanescent waves.

3.3 Wavenumber measurement

A steel beam with a thickness of $h = 0.0055\,m$ will be considered. The material properties are given by a Young's modulus $E = 2.1 \cdot 10^{11}\,Pa$ and a density $\rho = 7800\,kg/m^3$. Figure 3.1 shows the experimental set-up for the measurement of the wavenumber in a beam. Three transducers to measure lateral acceleration are attached to the beam a distance d apart. Their mass is small compared to the properties of the beam and therefore the wave motion isn't affected considerably. An electrodynamic shaker excites the beam. The distance between the excitation and the transducers is long enough so that the evanescent waves decay to a negligible amplitude. Since the beam is finite, both ends are damped in order to minimize the amplitudes of reflected waves. The assumption is made, that two time harmonic propagating waves in the positive and negative direction respectively are present at the accelerometers. Thus, the lateral displacement and acceleration are given by

$$w(x,t) = \left(a^+ e^{-ikx} + a^- e^{ikx}\right) e^{i\omega t} \tag{3.3.1}$$

$$a(x,t) = -\omega^2 \left(a^+ e^{-ikx} + a^- e^{ikx}\right) e^{i\omega t} \tag{3.3.2}$$

Substituting the locations of the accelerometers $(x_1 = -d, \quad x_2 = 0, \quad x_3 = d)$ gives

$$\begin{aligned} a_1(t) &= -\omega^2 \left(a^+ e^{ikd} + a^- e^{-ikd}\right) e^{i\omega t} \\ a_2(t) &= -\omega^2 \left(a^+ + a^-\right) e^{i\omega t} \\ a_3(t) &= -\omega^2 \left(a^+ e^{-ikd} + a^- e^{ikd}\right) e^{i\omega t} \end{aligned} \tag{3.3.3}$$

The beam is excited by a random signal and the frequency transfer functions A_1, A_2 and A_3 are determined. In the post-processing, the frequency spectra are combined such that

$$\begin{aligned} \frac{A_1 + A_3}{A_2} &= \frac{a^+ e^{ikd} + a^- e^{-ikd} + a^+ e^{-ikd} + a^- e^{ikd}}{a^+ + a^-} = e^{-ikd} + e^{ikd} \\ &= 2cos(kd) \end{aligned} \tag{3.3.4}$$

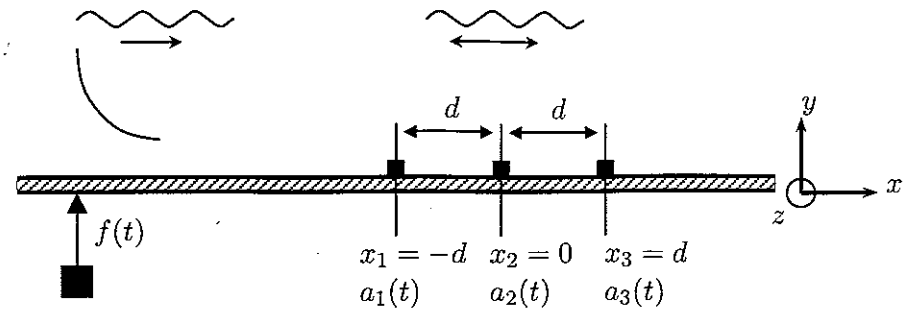

FIGURE 3.1: *Measurement set up*

With the assumption that the wavenumber is given by

$$k^2 = \omega\sqrt{\frac{\rho A}{EI}} = \omega\sqrt{\alpha}$$

the constant α can be found by fitting $cos(kd)$ to the measured data, as shown in Figure 3.2. The comparison of the analytical and finite element solutions with the measurement can be seen in Figure 3.3. While the finite element solution cannot be distinguished from the analytical solution, the curve obtained from experiment does differ slightly. This is primarily due to an inaccurate estimation of the dimensions and properties of the beam and also to the idealized beam model and to general measurement errors.

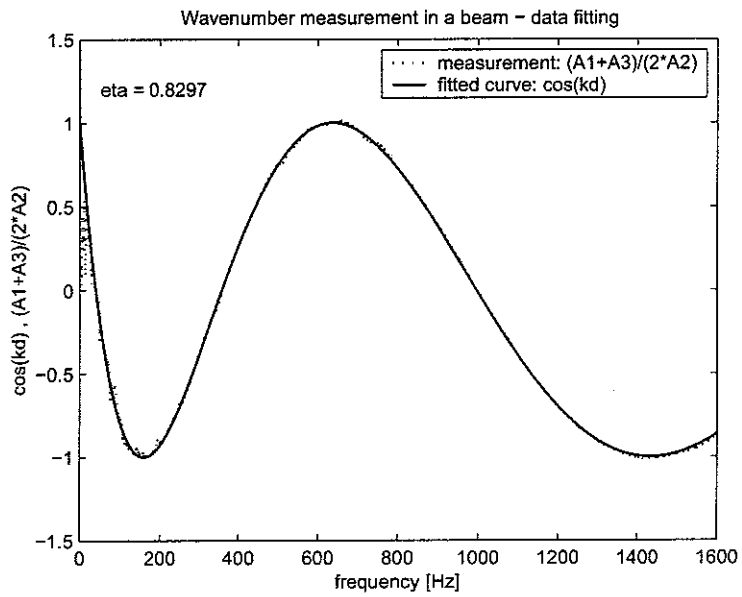

FIGURE 3.2: *Fitting of cos(kd) to the measured data*

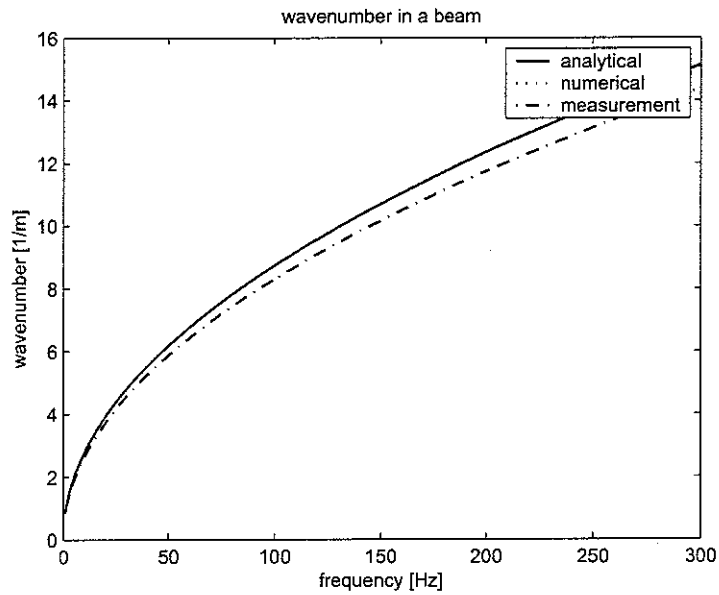

FIGURE 3.3: *Wavenumber curve for a beam - analytical and numerical solution and measurement*

4 WAVE PROPAGATION IN PLATES

In this section one-dimensional bending waves in flat uniform isotropic plates are considered. Although various types of waves can propagate in plates, bending waves are often of most interest, because they involve out of plane displacements. The dispersion relations will be derived from theory and compared with numerical results from the finite element analysis. ANSYS is used to obtain the mass and stiffness matrices of a cross-section. Structural damping will be neglected in order to present the numerical results in a more clear form. Post-processing of the system matrices is done in MATLAB.

4.1 Bending waves in free plates

4.1.1 Theory

Figure 4.1 shows a plate of thickness h in the z-direction and infinite dimensions in the (x, y)-plane. The bending wave equation in such a plate is (see Cremer [3], Fahy [1])

$$D\left(\frac{\partial^4 w}{\partial x^4} + 2\frac{\partial^4 w}{\partial x^2 \partial y^2} + \frac{\partial^4 w}{\partial y^4}\right) = -\rho h \frac{\partial^2 w}{\partial t^2} \tag{4.1.1}$$

where

$$D = \frac{Eh^3}{12(1-\nu^2)}$$

is the bending stiffness of the plate and rho its density. A solution to Equation 4.1.1 can be found in form of harmonic wave motion as

$$w(x, y, t) = e^{-ik_x x} e^{-ik_y y} e^{i\omega t} \tag{4.1.2}$$

where k_x and k_y are the wavenumbers of the wave-components in the x and y direction respectively. Substitution into Equation 4.1.1 and simplification gives

$$D(k_x^2 + k_y^2)^2 - \rho h \omega^2 = 0 \tag{4.1.3}$$

With $k_b^2 = k_x^2 + k_y^2$, the wavenumber of a free bending wave travelling in the (x, y)-plane of the plate can be expressed as

$$k_b^2 = \omega\sqrt{\frac{\rho h}{D}} = \omega\sqrt{\frac{12(1-\nu^2)\rho}{Eh^2}} \tag{4.1.4}$$

It can be noted that this wavenumber is similar to that for a bending wave in a beam, apart from the factor $(1 - \nu^2)$.

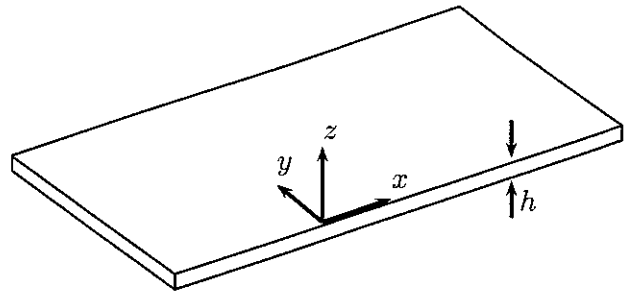

FIGURE 4.1: *Free plate*

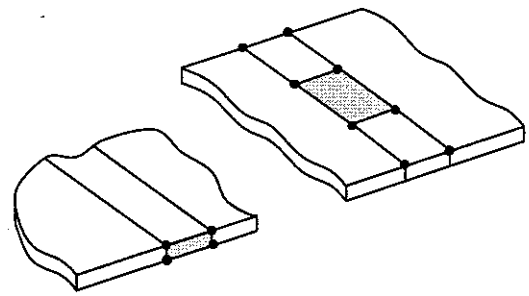

FIGURE 4.2: *Mesh of section by plain strain elements and shell elements*

4.1.2 Numerical results

First, the section of the waveguide that will be modelled in FEA has to be defined. The dimension of the direction of wave propagation has to be infinite. For the infinite plate the cross-section will therefore be infinite in one dimension and very small in the other direction. The simplest FE-mesh is a rectangular plane-strain element over the thickness h and with length Δ. For a finite plate, the wavenumber of a bending wave will be about the same as given in equation 4.1.4, as long as the width is large compared to the wavelength. In this case, the cross-section can be modelled by a number of shell elements with thickness h distributed over the width L. The use of plane-strain and shell elements is illustrated in Figure 4.2

Consider a steel plate with a thickness $h = 0.001\,m$ and a width $L = 1\,m$. The length of the section is chosen to be $\Delta = 0.01\,m$ and 50 elements will be used across the width. The structural model is assumed to be linear, isotropic, with Young's modulus $E = 2.1 \cdot 10^{11} Pa$, density $\rho = 7800\,kg/m^3$ and Poisson's ratio $\nu = 0.3$. Figure 4.3 shows the dispersion relations, whereby the numerical solution for the finite plate is compared to the analytical solution for an infinite plate and a beam. The wavenumber in a beam is slightly higher, because the lateral contraction is not prevented ($\nu = 0$) as it is the case in plane bending.

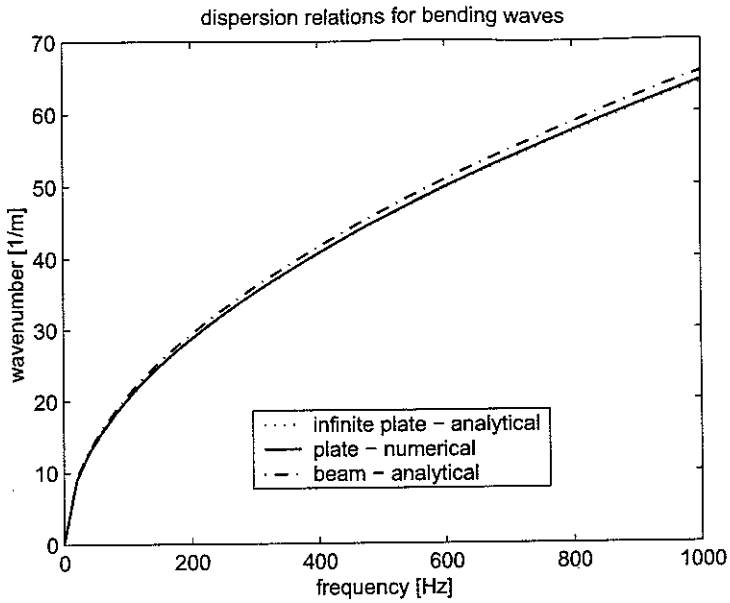

FIGURE 4.3: *Dispersion relations for bending waves in free plates and beams*

4.2 Bending waves in a simply supported plate strip

4.2.1 Theory

Figure 4.4 shows a finite plate strip of width L and thickness h that is simply supported along two edges. The boundary conditions along the edges are

$$w(x,0) = w(x,L) = 0 \tag{4.2.1}$$

$$\frac{\partial^2 w(x,0)}{\partial y^2} = \frac{\partial^2 w(x,L)}{\partial y^2} = 0 \tag{4.2.2}$$

A solution to equation 4.1.1 can be written in the form

$$w(x,y,t) = e^{-ik_x x} sin(k_y y) e^{i\omega t} \tag{4.2.3}$$

which satisfies the boundary conditions if

$$k_y = \frac{n\pi}{L}$$

There are characteristic displacements, referred to as modeshapes, over the width of the cross-section in the form of multiples of a half sine wave with discrete values of the wavenumber. Thus

$$w(y) = sin(k_y y) \quad \text{with} \quad k_y = \frac{n\pi}{L} \quad \text{for} \quad n = 1,2,3,\ldots \tag{4.2.4}$$

In order to find the wavenumber of the waves travelling in the x-direction, we can substitute k_y into equation 4.1.3 and solve for k_x, which gives

$$k_{b_n}^2 = k_{x_n}^2 = \pm\omega\sqrt{\frac{\rho h}{D}} - \left(\frac{n\pi}{L}\right)^2 \quad \text{for} \quad n = 1,2,3,\ldots \tag{4.2.5}$$

The number of wavenumbers k_n is infinite, their values however are discrete since they are associated with the mode shapes as defined in equation 4.2.4. Because the wavenumber k is real for propagating waves, from equation 4.2.5 it follows that there must be a minimum frequency for the nth wave to start propagating. This frequency is called the cut-on frequency and is given for the nth wavemode by

$$\omega_{0_n} = \sqrt{\frac{D}{\rho h}} \left(\frac{n\pi}{L}\right)^2 \tag{4.2.6}$$

The cut-on phenomenon can be compared to the condition that the wavenumber of a bending wave propagating in a free plate is just large enough such that kL is a multiple of π. In terms of the eigenvalues, the cut-on condition is satisfied when the magnitude of λ equals one. At the cut-on frequency, $\lambda = 1$ and from equation 2.3.12 it follows that $\mu = 0$ and $k = 0$.

The group velocity is defined as

$$c_g = \frac{\partial \omega}{\partial k} \tag{4.2.7}$$

Taking the derivative of equation 4.2.5 with respect to ω gives

$$\frac{\partial k_n}{\partial \omega} = \frac{1}{2} \frac{\sqrt{\frac{\rho h}{D}}}{\sqrt{\omega \sqrt{\frac{\rho h}{D}} - \left(\frac{n\pi}{L}\right)^2}} = \frac{\sqrt{\frac{\rho h}{4D}}}{k_n} \tag{4.2.8}$$

It follows that the group velocity for the nth wave is given by

$$c_{g_n} = \frac{\partial \omega}{\partial k_n} = \sqrt{\frac{4D}{\rho h}}\, k_n \tag{4.2.9}$$

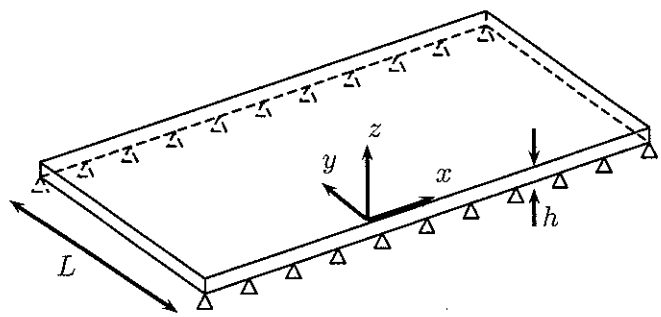

FIGURE 4.4: *Simple supported plate*

4.2.2 2-element-mesh

Consider a simply supported steel plate as in Figure 4.4 which is meshed by two elements over the width of the cross-section, which hence has a limited number of

degrees of freedom. The thickness is $h = 0.001\,m$ and the length of the section is chosen to be $\Delta = 0.01\,m$. As equation 4.2.6 shows, the width L of the plate has a strong influence on the cut-on frequency and in general the wider the plate the more waves and modes appear in a certain frequency range. With the objective of using two finite elements only, a width of $L = 0.3\,m$ is chosen. Two rectangular shell elements are used to mesh the cross-section with nodes at $y = 0$, $y = L/2$ and $y = L$ respectively, which gives 6 nodes overall. The mass and stiffness matrices can be obtained by performing a dynamic simulation in ANSYS. In general, there are 6 degrees of freedom per node, therefore the system matrices will be of size 36×36. Since the interest is only in bending, all degrees of freedom describing in-plane motion can be neglected. The associated rows and columns in the system matrices are removed, which reduces them to size 18×18. Furthermore, the boundary conditions at $y = 0$ and $y = L$ are applied by removing the associated rows and columns from the mass and stiffness matrices. The remaining degrees of freedom are

$$w, \quad \frac{\partial w}{\partial x}, \quad \begin{array}{ll} \frac{\partial w}{\partial y} & \text{at} \quad y = 0, \\ \frac{\partial w}{\partial y} & \text{at} \quad y = L/2, \\ \frac{\partial w}{\partial y} & \text{at} \quad y = L \end{array} \tag{4.2.10}$$

Since there are nodes on the left and the right border of the section, there is a total of 10 degrees of freedom left, resulting in 10×10 mass and stiffness matrices. In order to build up the transfer matrix, the global node numbering has to be as shown in Figure 4.5, beginning on a corner on the left and ending at the opposite corner on the right. In general, the global node numbering in ANSYS is different, therefore appropriate rearrangement of rows and columns of the system matrices has to be done.

Solving the eigenvalue problem (2.3.2) gives five pairs of eigenvalues and five pairs of eigenvectors for each frequency. Figure 4.6 shows the location of the eigenvalues in the complex λ-plane, Figure 4.7 shows their location in the complex (μ, k)-plane, each for four selected frequencies. A description of these Figures can be found in Table 4.2 and Table 4.3 respectively. The wavenumbers of the first and second wave are shown as functions of frequency in Figure 4.8, with the analytical and numerical solutions being compared. The wavenumber of the first wave is estimated very accurately, the second wavenumber differs from the analytical solution, which is due to the use of only two elements and a poor width-to-height ratio of the elements. Figure 4.9 shows the improvement in the estimation of the second wavenumber when the number of elements is increased. Energy related quantities are presented in Figure 4.10. The peaks in the energy and power-flow curves at the cut-on frequency of each wave represent resonance. The numericaly estimated group velocities are compared to the analytical solutions and the results agree very well.

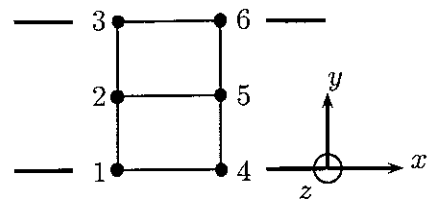

FIGURE 4.5: *two-element-mesh*

4.2.3 50-element-mesh

As a further example, the steel plate from section 4.1.2, with thickness $h = 0.001\,m$ and width $L = 1\,m$, is modelled. The length of the section is chosen as $\Delta = 0.01\,m$ and 50 rectangular shell elements are used to describe the cross-sectional displacement, resulting in 612 nodal degrees of freedom. The mass and stiffness matrices are then rearranged to order the global node numbers in the required way. Neglecting the in-plane motion and applying the boundary conditions reduces the system to 298 degrees of freedom. Figure 4.11 shows the location of eigenvalues in the complex (μ, k)-plane at $60Hz$. There are 8 eigenvalues on the imaginary axis, which can be identified as propagating waves, 4 of them in each direction. The 5th wave is close to cut-on. There are some eigenvalues on the real axis that represent evanescent waves. The complex eigenvalues are attenuating waves.

An algorithm finds the eigenvalues representing propagating waves and the associated eigenvectors. Additionally, the path of the eigenvalues before they reach $|\lambda| = 1$ is determined, which gives an imaginary wavenumber before cut-on. Since the eigenvalues with $|\lambda| \lesseqgtr 1$ change their position with frequency, it is hard to trace them. However it is possible to identify them using the eigenvectors. The algorithm uses a criterion analogous to the modal assurance criterion (MAC) to compare the eigenvectors before and after a frequency step. It is defined as

$$MAC_{\omega-1,\omega} = \frac{\left| \left(\mathbf{q}_{L_{\omega-1}}^H \, \mathbf{q}_{L_\omega} \right) \right|^2}{\left(\mathbf{q}_{L_{\omega-1}}^H \, \mathbf{q}_{L_{\omega-1}} \right) \left(\mathbf{q}_{L_\omega}^H \, \mathbf{q}_{L_\omega} \right)} \tag{4.2.11}$$

Depending on the application and the size of the frequency step, the eigenvector of an eigenvalue will usually change only slightly or not at all from one frequency to another, which gives a correlation coefficient (MAC) of nearly one. With this method, the eigenvalues can be clearly identified at each frequency. Figure 4.12 shows the first 5 wavenumbers, before and after cut-on, for the plate. In Figure 4.13 the eigenvectors of the first 5 propagating waves are plotted against the node number across the strip. As expected, the modeshapes are multiples of a half sine wave.

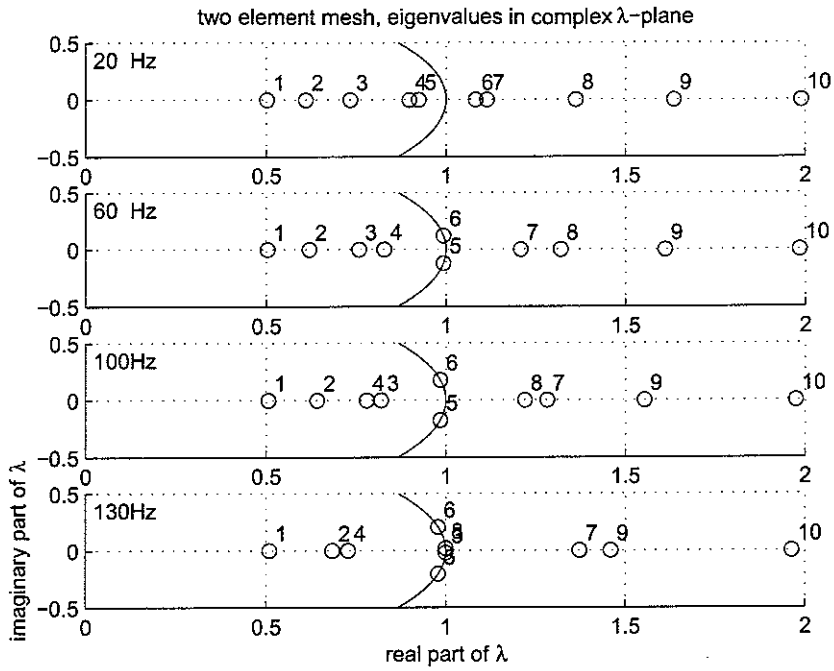

FIGURE 4.6: *Eigenvalues in complex λ-plane*

Figure 4.6

$f = 20$Hz:	all eigenvalues (ev.) are real, no propagating waves ev. 1-5 ($\|\lambda_j\| \leq 1$) describe waves going in the positive direction ev. 6-10 ($\|\lambda_j\| \geq 1$) describe waves going in the negativ direction
$f = 60$Hz:	ev. 5 and 6 become complex and lie on the unit circle ($\|\lambda_j\| = 1$)
$f = 100$Hz:	ev. 5 and 6 move around the unit circle ev. 3 and 8 move towards $\|\lambda_j\| = 1$
$f = 130$Hz:	ev. 3 and 8 also become complex and lie on the unit circle

TABLE 4.2: Description of Figure 4.6

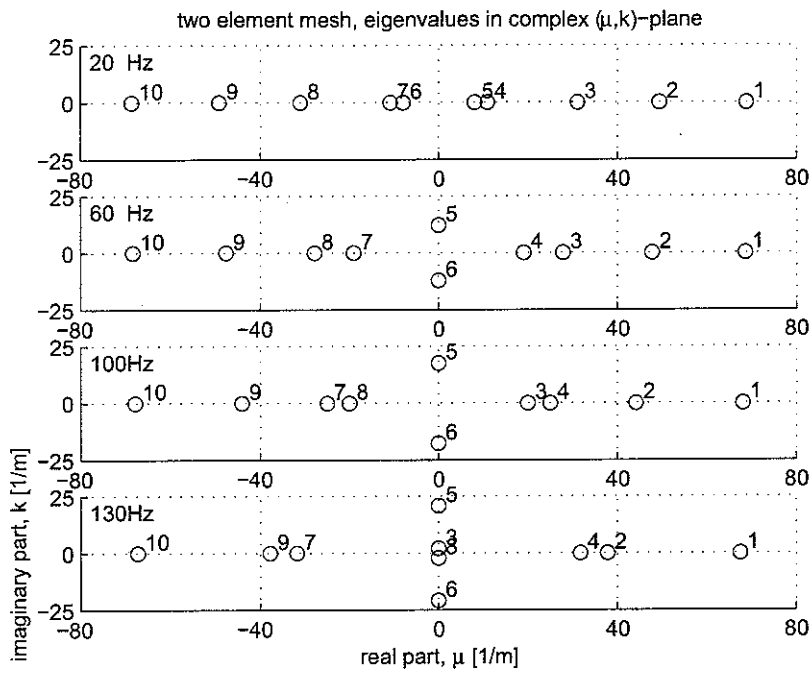

FIGURE 4.7: *Eigenvalues in complex* (μ, k)*-plane*

Figure 4.7

$f = 20$Hz:	$k_j = 0, \quad \mu_j \lesseqgtr 1$ no real wavenumber, no oscillation, only evanescent waves
$f = 60$Hz:	$(k_5 > 0, \quad \mu_5 = 0)$ propagating wave in the positive direction $(k_6 < 0, \quad \mu_6 = 0)$ propagating wave in the negative direction
$f = 100$Hz:	$(\lvert k_5 \rvert, \quad \lvert k_6 \rvert)$ increase with frequency
$f = 130$Hz:	$(k_3, \quad k_8)$ second wavemode cuts on

TABLE 4.3: Description of Figure 4.7

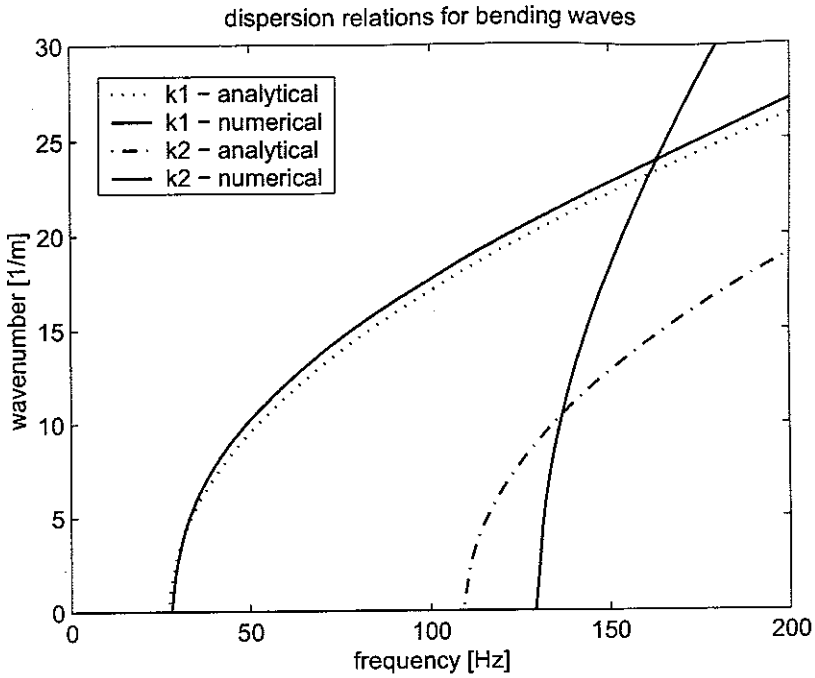

FIGURE 4.8: *Dispersion relations for bending waves in a simply supported plate strip*

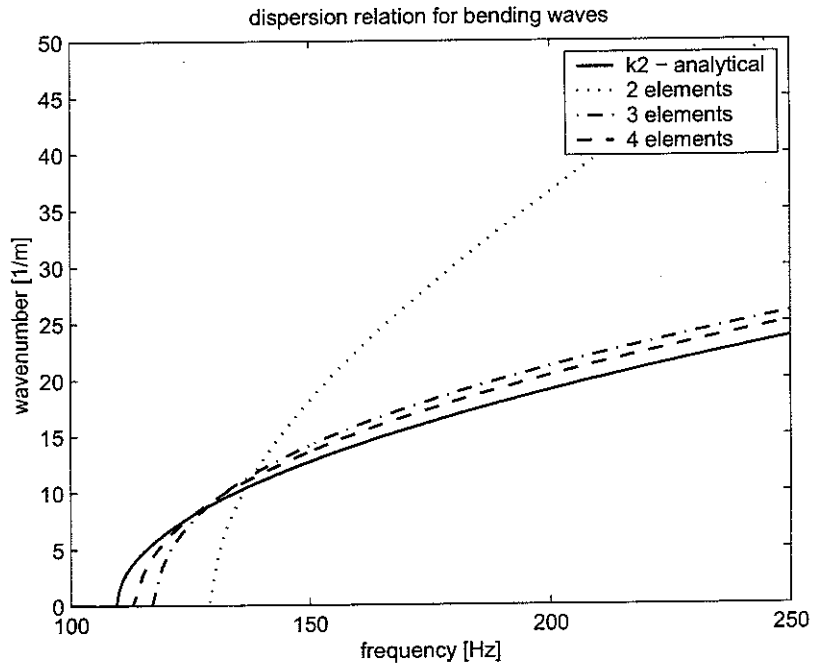

FIGURE 4.9: *Improved wavenumber estimation with higher number of elements*

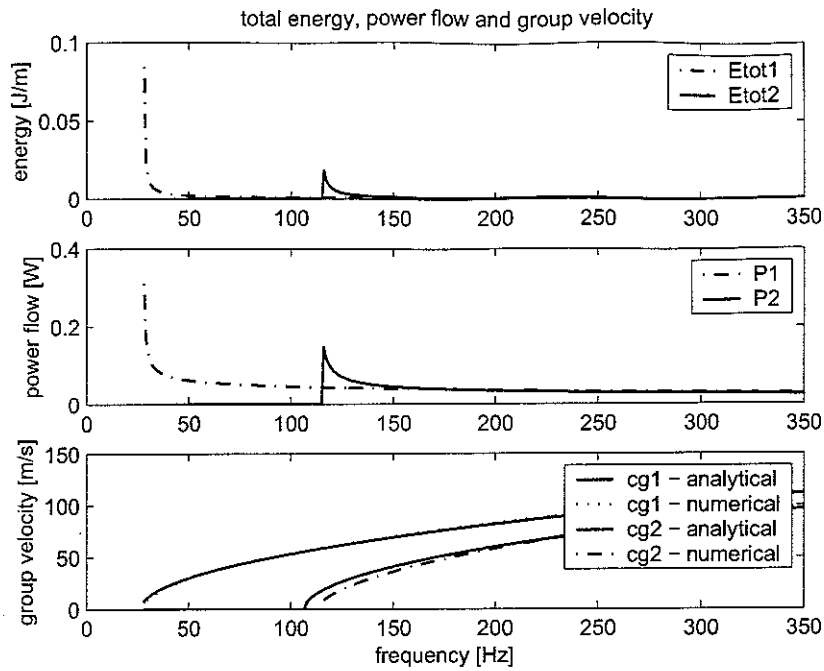

FIGURE 4.10: *Total energy per unit length $\bar{E}_{tot}$, power-flow $\bar{P}$ and group velocity c_g for the first two waves in a simply supported plate strip*

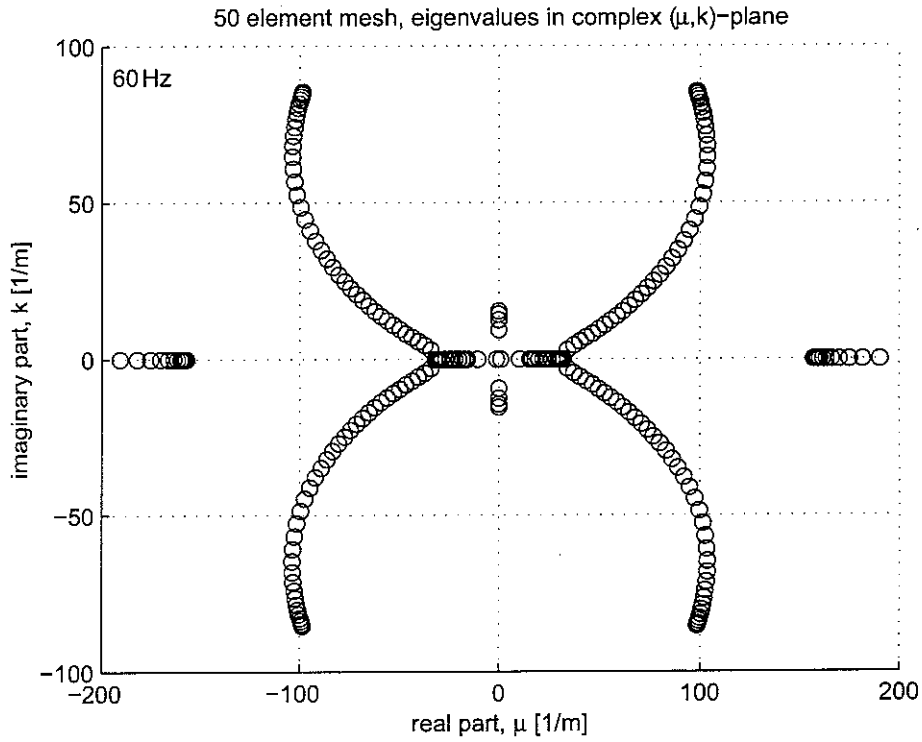

FIGURE 4.11: *Eigenvalues in complex (μ, k)-plane*

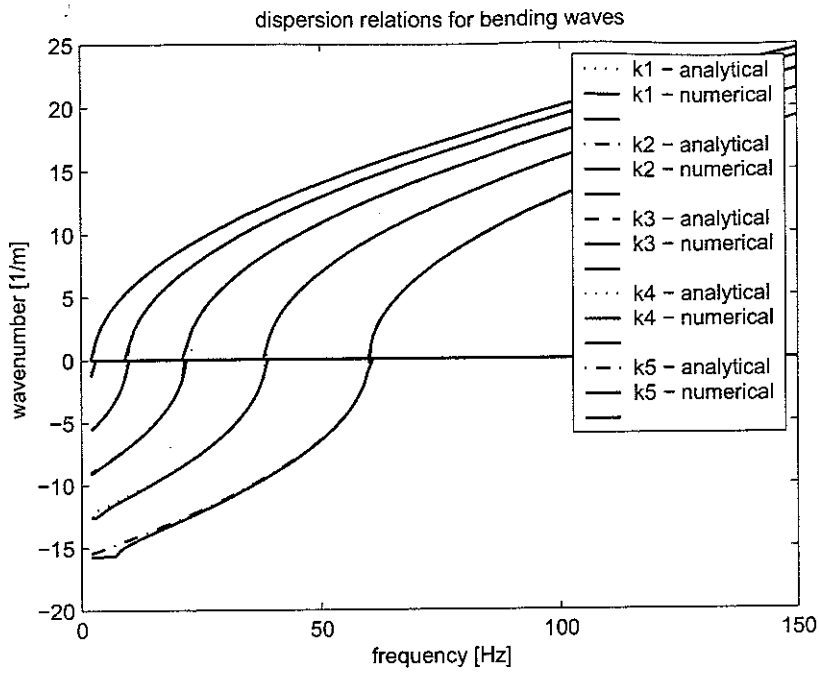

FIGURE 4.12: *Dispersion relation for bending waves in a simple supported plate*

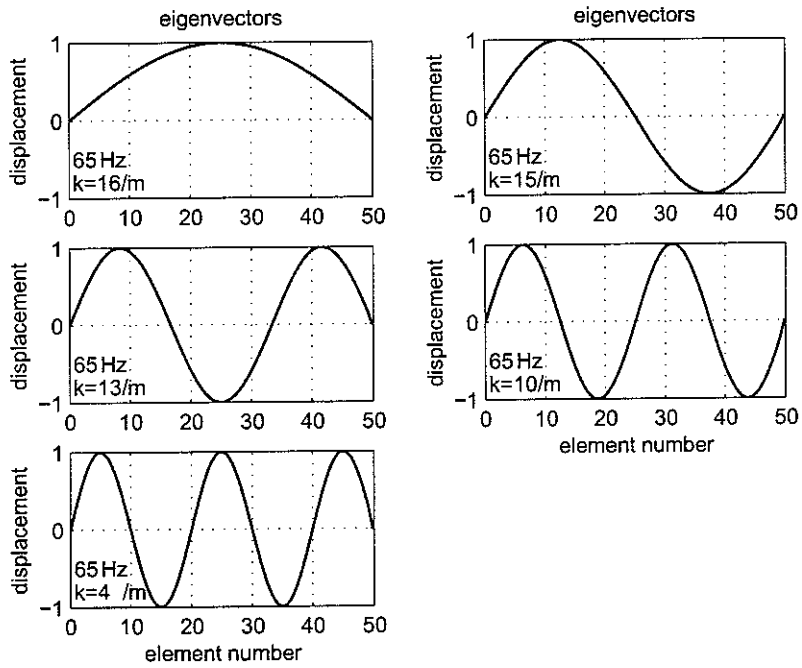

FIGURE 4.13: *Mode shapes of bending waves in a simply supported plate strip*

5 WAVE PROPAGATION IN LAMINATED PLATES

5.1 FE-modelling of a laminated plate

The transfer matrix approach will be used to calculate the wavenumbers and the wavetypes in a laminated plate. A symmetric sandwich panel with a $15\,mm$ thick core and $0.6\,mm$ thick skins on both sides is considered. Other dimensions are infinite and there are no boundary conditions. The material properties of the core are those of a linear elastic isotropic material with Young's modulus $E = 3 \cdot 10^7 Pa$, density $\rho = 48\,kg/m^3$ and Poisson's ratio $\nu = 0.2$. The skins are of Aluminium with properties given by $E = 7.1 \cdot 10^{10} Pa$, $\rho = 2700\,kg/m^3$ and $\nu = 0.3296$. Figure 5.1 shows the finite element mesh of the cross-section that describes the displacement field over the thickness h. Rectangular plain strain elements were used, one each to mesh the skins and fifteen to mesh the core, giving a total of seventeen elements. The elements have two nodal degrees of freedom, a displacement in the direction of wave propagation x and a displacement in the z direction. Therefore the in-plane and the out-of-plane motions of the cross-section are described by linear functions between the nodes. The dispersion curves will be calculated for frequencies up to $40\,kHz$. The length Δ of the cross-section is $\Delta = 0.001\,m$, which gives good accuracy for wavenumbers up to about $k = 1000/m$.

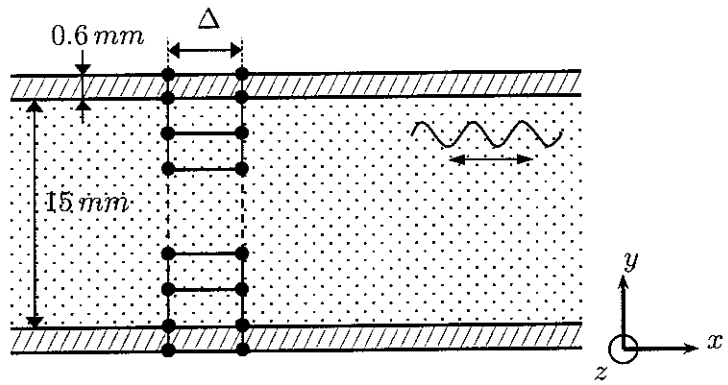

FIGURE 5.1: *Mesh of the cross-section of a laminated plate*

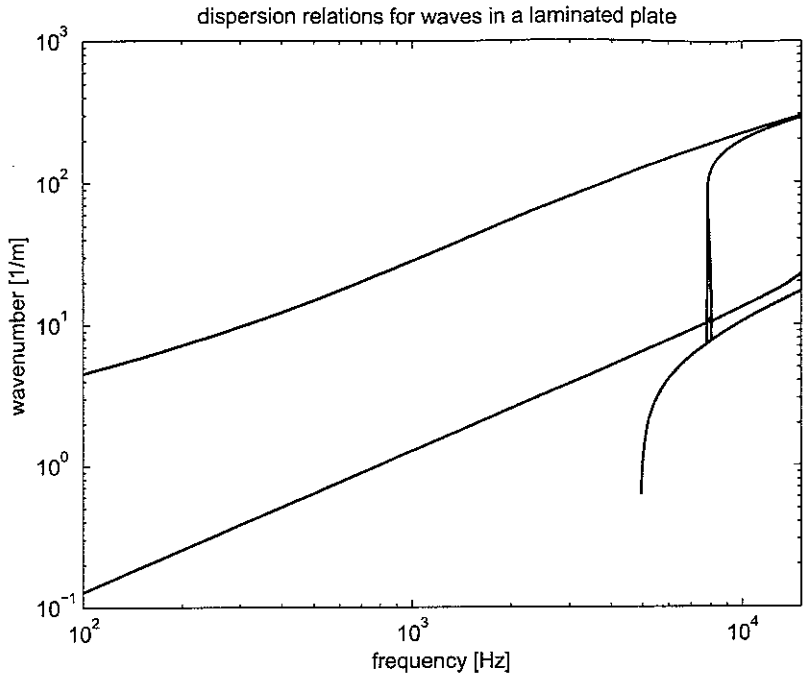

FIGURE 5.2: *Dispersion relations for waves in a laminated plate up to 15 kHz*

5.2 Dispersion relations

The wavenumbers are shown in Figure 5.2 and Figure 5.3. Below $5\,kHz$, two propagating waves exist. Extensional waves and bending waves in this isotropic plate appear as straight lines on the log-log plot of Figure 5.2. While the lower line seems to be straight, the upper line shows some curvature, which could refer to a change of the modeshape. At $5\,kHz$ a third propagating wave cuts on and at about $8\,kHz$ a 4th wave appears with a real nonzero wavenumber. This phenomenon is considered in detail in the next section. At $18\,kHz$ the a fifth wave cuts on and at $28\,kHz$ a sixth wave appears.

5.3 Cut on with nonzero wavenumber

Figure 5.4 shows the dispersion curves between $7600\,Hz$ and $8200\,Hz$. Above $5000\,Hz$, three waves (a, b, c) exist. At $7810\,Hz$ two waves (d, e) cut on with the same finite nonzero wavenumber. While the wavenumber of wave d increases, the wavenumber of wave e decreases, which means that the wave has a negative group velocity. Therefore it is a wave going in the negative direction, but with a positive wavenumber. At $8016\,Hz$, the wavenumbers of wave e and b have the same value and both waves disappear, meaning they become attenuating waves and no longer propagate. At $8039\,Hz$, two more waves f and g cut on with the same nonzero wavenumber. While wave g only seems to exists over a frequency range of $1 - 2\,Hz$, wave f is stable and has an increasing wavenumber.

Now it will be demonstrated how a plot showing the location of the eigenvalues in the complex λ-plane can be used to obtain more detailed information. The frequency range from $8015\,Hz$ to $8040\,Hz$ will be considered and the critical eigenvalues are

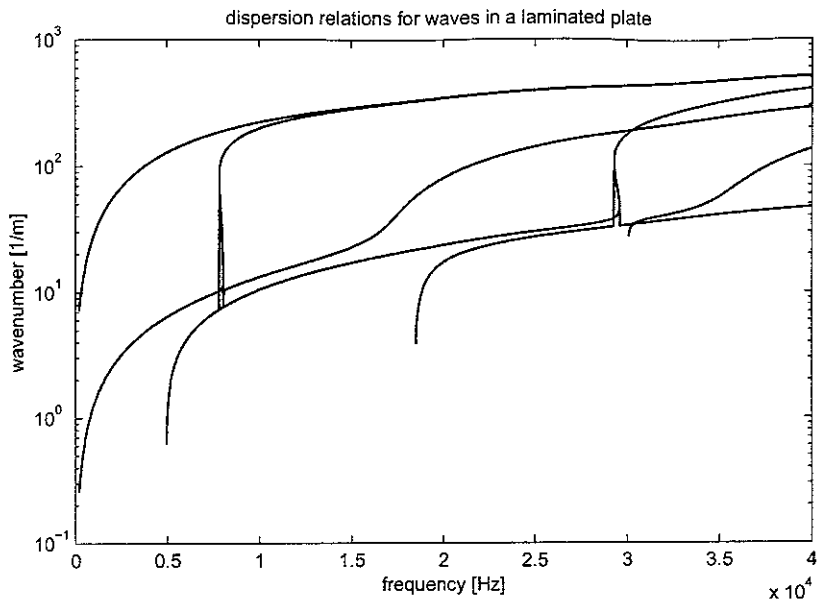

FIGURE 5.3: *Dispersion relations for waves in a laminated plate up to 40 kHz*

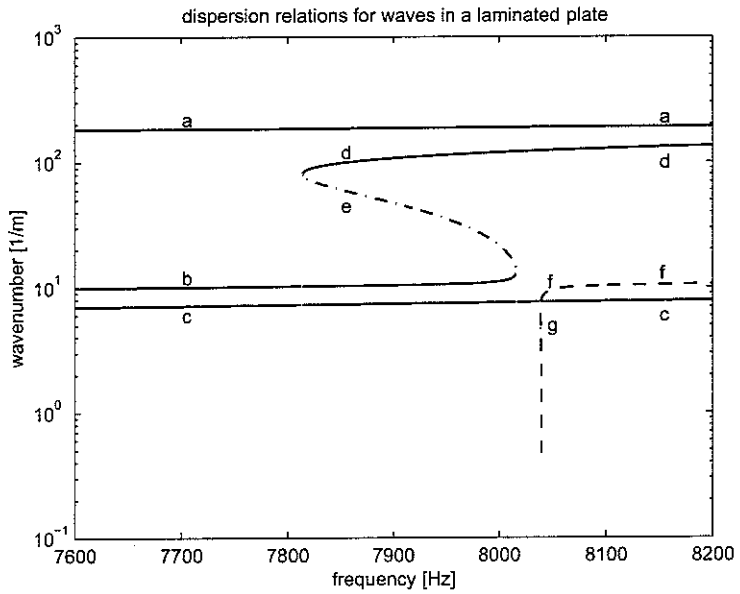

FIGURE 5.4: *Wavenumbers of a laminated plate in a frequency range from 7600 Hz to 8200 Hz*

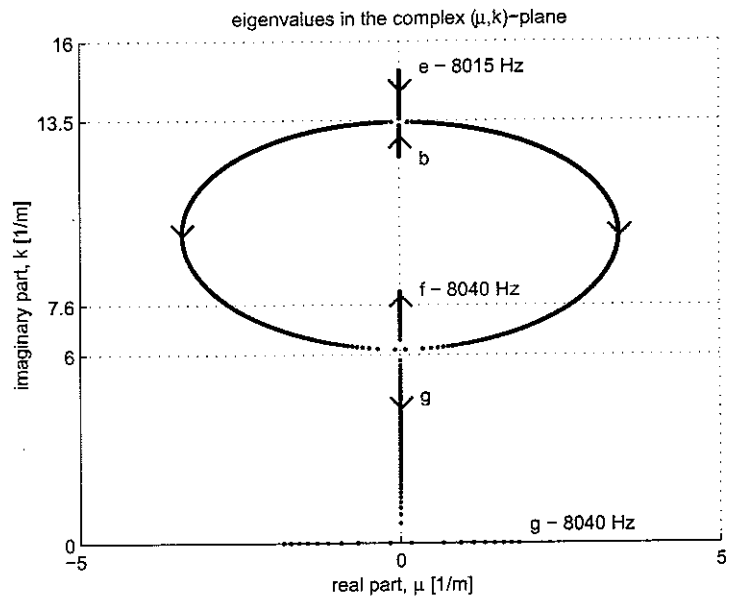

FIGURE 5.5: *Location of eigenvalues in complex λ plane in the frequency span from 8015 Hz to 8040 Hz*

shown in Figure 5.5.

The eigenvalues are plotted with a frequency step of $1\,Hz$. Eigenvalues e and b move along the imaginary axis towards each other. They leave the imaginary axis at the same point ($8016\,Hz$), one with a positive real part, the other with a negative real part. After the real parts increase for about $15\,Hz$, they then begin to decrease. At $8039\,Hz$ the eigenvalues become purely imaginary again and show up as propagating waves f and g on the wavenumber plot. Eigenvalue f moves up the imaginary axis, but g becomes purely real and this wave becomes evanescent.

The phenomena of waves appearing with finite nonzero wavenumbers, waves with decreasing wavenumbers and wave pairs that coalesce are quite unusual. However Figure 5.3 shows that these phenomena repeat at about $32\,kHz$. Similar results have be found by an alternative approach using spectral elements by Shorter [14].

The effects of a change in the material properties on the dispersion relations have been studied and the density of the core material seemed to have strong influence on the wavenumber curves. Figure 5.6 shows the dispersion curves for an increase in the density of the core by a factor of 10.

5.4 Modeshapes and wavetypes

The modeshape of a wave is characterized by in-plane (x) and out-of-plane displacements. The eigenvectors can be decomposed in a set of 50 nodal x and y displacements respectively, giving a spatial variation with x and y for each modeshape. While

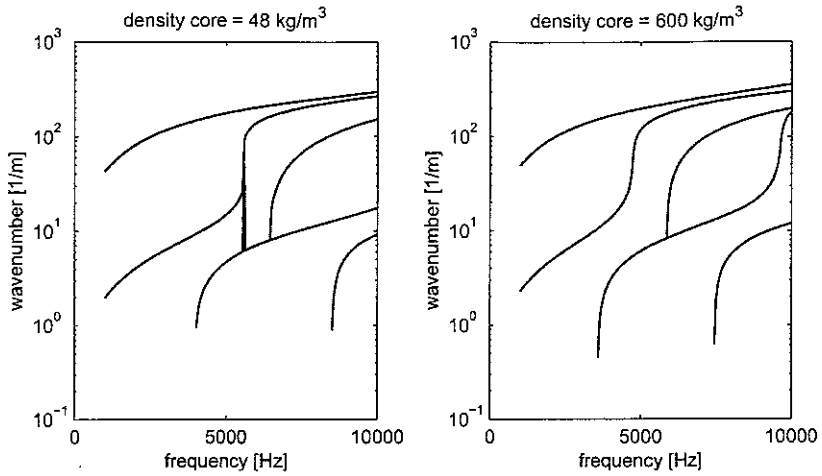

FIGURE 5.6: *Wavenumbers for different values of density of the core material of a laminated plate.*

the y displacements are real valued, the displacements in the x-direction are purely imaginary, since it is in the direction of wave propagation.

In Figure 5.7, the x and y shapes of the first three waves (a, b, c) at about 7000 Hz can be seen (normalized to an amplitude of one). Wave a seems to be a bending wave, since the cross-section moves up and down in the out of plane direction. At the same time, there is some shear motion in the skins and in the core. Wave b is an extensional wave, with compression and extension in the x-direction and associated lateral contraction. Wave c is characterized by an out of phase motion of the skins in the x-direction, which is adopted by the core. Additionally, there is some bending like motion in the cross-section.

Figure 5.8 shows the modeshaps at 7900 Hz, after two more waves cut on with nonzero wavenumbers, with 5 waves now being present. The new propagating waves d (positive direction) and e (negative direction), are characterized by an extensional wave motion in the core including lateral contractions. The skins adopt this motion and themselves show only some small shear motion.

Finally, the modeshapes of the four waves at 9000 Hz are presented in Figure 5.9. After the extensional wave b disappeared at 8016 Hz it seems now to be similar to the wave mode f.

While the main characteristics of a wave remain the same over a large frequency range, the proportions seem to change quickly as frequency changes.

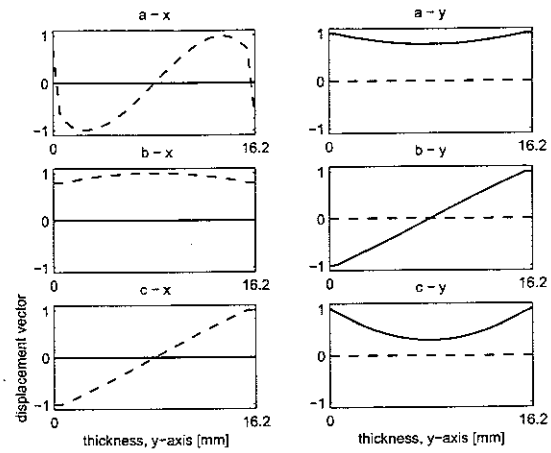

FIGURE 5.7: *Modeshapes of waves in a laminated plate at 7000 Hz*

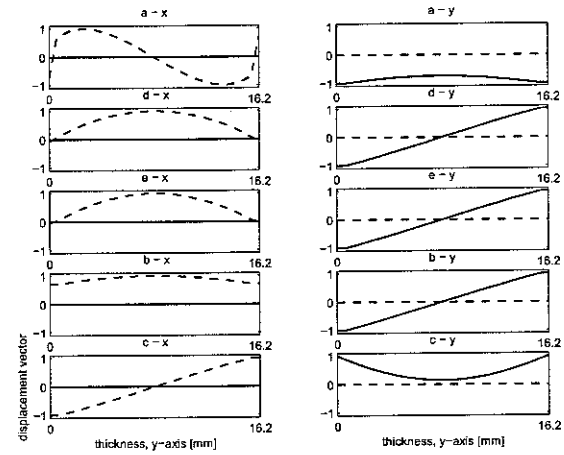

FIGURE 5.8: *Modeshapes of waves in a laminated plate at 7900 Hz*

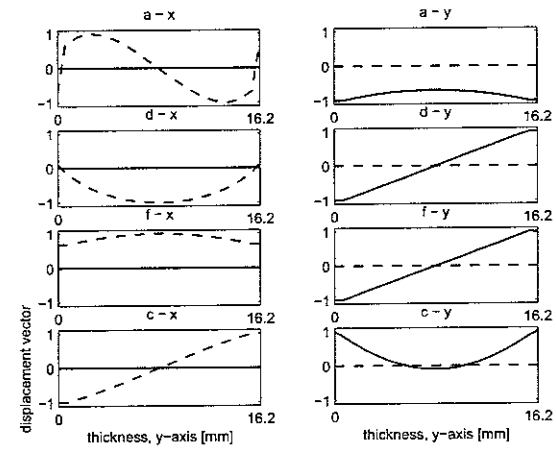

FIGURE 5.9: *Modeshapes of waves in a laminated plate at 9000 Hz*

5.5 Energy related quantities

The total energy, the power-flow and the group velocity have been calculated for the first three propagating waves up to $8\,kHz$ and are plotted in Figure 5.10. The results of wave a vary substantially with frequency, which could be compared to the curvature of the dispersion line, observed in section 5.2. The power-flow and the group velocity of wave b show a rapid decay after $8\,kHz$, which agrees with the fact that this wave is close to cut-off. The energy related quantities of wave c show a resonance peak at the cut-on frequency.

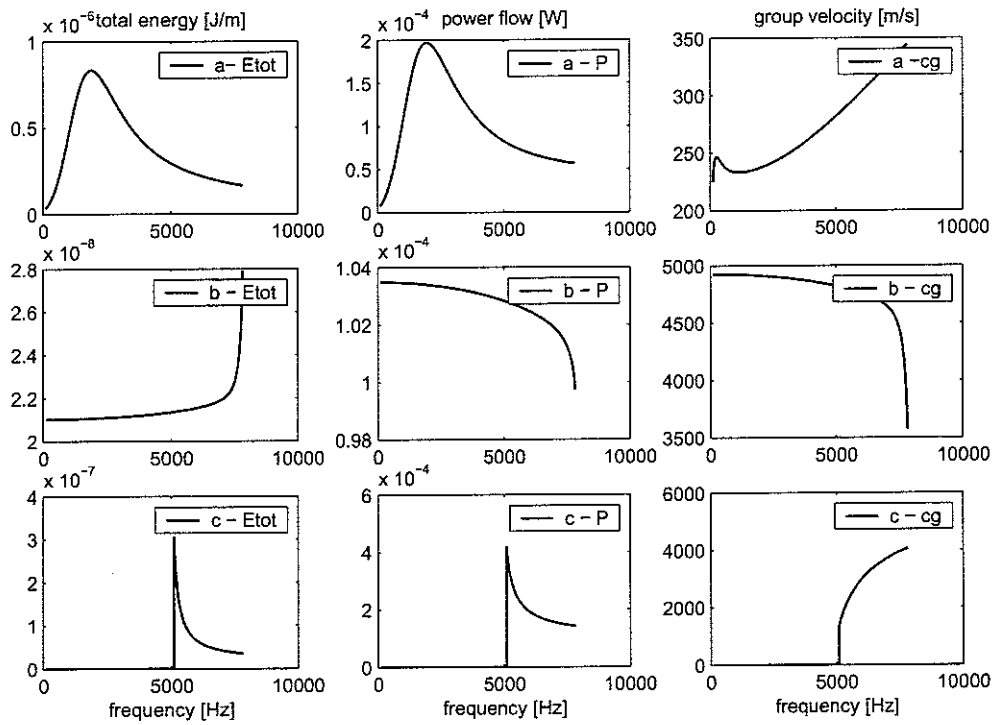

FIGURE 5.10: *Total energy per unit length $\bar{E}_{tot}$, power-flow $\bar{P}$ and group velocity c_g of waves in a laminated plate*

CONCLUDING REMARKS

In this report, a method to calculate wave propagation characteristics in uniform waveguides was presented. Firstly, the commercial FE package ANSYS is used to model a section of the waveguide. Then, the mass, stiffness and damping matrices are post-processed in MATLAB. The dynamic stiffness matrix is found, partitioned and rearranged to find the transfer matrix, which links the displacements and forces on both sides of the section. The propagation constants and the wavetypes are given by the eigenvalues and eigenvectors of the transfer matrix respectively. It has been shown, how a physical interpretation of the eigenvalues can be easily made by looking at their location in different complex planes. The dispersion relations for real and imaginary wavenumbers were found. Using the FE-formulation, the determination of wavetypes and the calculation of energy related quantities, i.e. the group velocity, are straightforward.

The method has been applied to examples of a rod, beam, plate strip and a laminated plate. When possible, numerical and analytical solutions have been compared, whereby no substantial differences occurred. The example of a laminated plate let to interesting and important results, which proofed the ability and usefulness of the approach.

The major advantage of the method is, that the full power of finite element libraries in standard FE packages can be used to mesh a general cross-section. The computational cost only depends on the size of the finite element mesh of the cross-section. The post-processing algorithm is stable and can be made generic for a given range of applications.

Future work is the advancement of the post-processing algorithm to increase the range of applications, for example to waveguides with rotational symmetry and a circular axis of wave propagation. A general generic code, together with widely spread and well known FE-packages could be used easily by a large number of people.

References

[1] F. Fahy, Sound and structural vibration, Academic Press, London, 1985

[2] L. Cremer, M. Heckl, Körperschall, Springer Verlag Berlin, 1996

[3] L. Cremer, M. Heckl, Structure borne sound, Springer Verlag Berlin, 1988

[4] R. Lyon, Statistical Energy Analysis of Dynamical Systems, MIT Press, 1975

[5] F. Fahy, Statistical Energy Analysis: a critical overview, Phil. Trans. R. Soc. Lond. A 346, 429-554, 1994

[6] M. Ohlrich, Structure-borne sound and vibration, Acoustic Technology, Note no 7022, DTU, August 2002

[7] A.H. von Flotow, Disturbance propagation in structural networks, Journal of Sound and Vibration 106, 433-450, 1986

[8] L. Brillouin, Wave propagation in periodic structures, New York: Dover, 1953

[9] D.J. Mead, Wave propagation in continuous periodic structures: research contributions from Southampton 1964-1995, Journal of Sound and Vibration 190, 495-524, 1996

[10] R.S. Langley, Analysis of power flow in beams and frameworks using the direct-dynamic stiffness method, Journal of Sound and Vibration 136(3), 439-452, 1990

[11] J. Doyle, Wave propagation in structures: an FFT-based spectral analysis methodology, Springer Verlag, 1989

[12] S. Finnveden, Finite element techniques for the evaluation of energy flow parameters, Proceedings of NOVEM, Lyon, 2000

[13] C.M. Nilsson, Waveguide finite elements for thin-walled structures, Licentiate thesis, KTH Stockholm, 2002

[14] P.J. Shorter, Wave propagation and damping in linear viscoelastic laminates, Journal of the Acoustical Society of America, Submitted for puplication

[15] L. Gry, Dynamic modelling of railway track based on wave propagation, Journal of Sound and Vibration 195, 477-505, 1996

[16] J.F. Allard, Propagation of sound in porous media, Elsevier, 1993

[17] A.Y.A. Abdel-Rahman, Matrix analysis of wave propagation in periodic systems, PhD thesis, University of Southampton, 1979

[18] D.J. Thompson, Wheel-rail noise generation, part III: Rail vibration, Journal of Sound and Vibration 161, 421-446, 1993

[19] D. Duhamel, B.R. Mace, M.J. Brennan, Finite element analysis of the vibrations of waveguides and periodic structures, ISVR Technical Memorandum No: 922, August 2003

[20] M. Petyt, Introduction to finite element vibration analysis, Cambridge University Press, 1990